Spring 2023

Detecting Physiological Concentrations of Alzheimer's Associated Amyloid-β Protein Utilizing a Cell-Based Response

Brittany Elizabeth Watson

Detecting Physiological Concentrations of Alzheimer's Associated Amyloid-β Protein Utilizing a Cell-Based Response

by

Brittany Elizabeth Watson

Bachelor of Science
University of Mississippi, 2018

Submitted in Partial Fulfillment of the Requirements

For the Degree of Doctor of Philosophy in

Biomedical Engineering

College of Engineering and Computing

University of South Carolina

2023

Accepted by:

Melissa A. Moss, Major Professor

Chandrashekhar Patel, Committee Member

Seongtae Bae, Committee Member

Chang Liu, Committee Member

Cheryl L. Addy, Interim Vice Provost and Dean of the Graduate School

Dedication

This dissertation work is dedicated to the memory of Mr. Rick Passman, who passed away from Alzheimer's disease, and his family. Mrs. Judi, Jake, and Bert, through the past 5 years working on this project, you all and Mr. Rick have been my motivation. It is my hope that this research will contribute to further diagnostics and understanding for this devastating disease.

Acknowledgements

First and foremost, I would like to thank my family. The support that I have received through this process is immeasurable. Mom and Dad, you made me who I am and have encouraged me to do everything I've set my mind to. Thank you for reading all my drafts and listening to my presentations. To my brothers and sister, Brandt, Blass, and Haley, you're always there when I need you. Now, let's go on a vacation! Aunt Pam and Uncle Bill, this all started when I walked into your kitchen and said, "I want to go to grad school." You have been there from the start. Can you believe we are here? To my grandparents, I have been blessed to have you all in my life. Papa, I wrote the bulk of this next to your side. I know you're watching in the sky to see how it all turns out.

I wouldn't be here without the constant encouragement from all of you. Thank you for celebrating all the wins, big and small. I hope to make you proud.

To my dear friends, near and far, you have helped me along the way. What a blessing it is to have you all in my life. Taylor, Caroline, Skylar, Colton, Nathan, Jenny, Nolan, Candice, Jane, Brenna, Cole, and Paige, y'all have made South Carolina so fun. I will forever cherish all we have shared together. Leigh, thanks for always listening to how the cells were doing, and making sure life stayed fun even from far away. Aly, Alex, Anna, Madison, Marissa, thank you for always cheering me on. Kachet and Don, my SC mom and brother, I am so thankful for you. Thank you to Dr. Dwight Waddell, who encouraged me to get here.

I want to thank Dr. Melissa Moss for her mentorship and continuous support. Dr. Moss welcomed me into her lab and has guided and challenged me to become the researcher I am today. She has supported my ideas and filled in the gaps when I can't quite finish a sentence. I could not have had a better mentor. I would also like to thank Dr. Mark Uline for his constant support and mentorship. Thank you to my committee, Dr. Shekar Patel, Dr. Seongtae Bae, and Dr. Chang Liu, from whom I have learned so much. Thank you to Vernon, Kachet, and Kimberly who make things happen daily and always keep me in check. To my undergraduate mentees, who have become my friends, Shannon, Julia, Nolan, I have learned more from teaching you than I ever could have alone. I am proud of you all.

I never thought I would be the person to do this, but thank you to my sweet pup Cooper, who has accompanied me to campus this past year more than anyone else (Thanks, Dr. Moss for letting me bring him).

I could write another whole dissertation on all the people that have helped me along the way. I am so incredibility thankful for my support network. Lastly, thank you to the Biomedical Engineering Program here at USC. I am so thankful for the opportunities and experiences the BMEN program has allowed me to be a part of.

Abstract

Alzheimer's disease (AD) is characterized symptoms of cognitive impairment resulting from blood-brain barrier (BBB) breakdown and neuronal cell death. AD is associated with aggregated amyloid-β (Aβ) plaques deposited around brain vasculature and within the brain. Changes in the brain occur up to 20 years before symptoms arise; however, there is currently no pre-symptomatic detection method available for AD. An intact BBB requires tight junction proteins (TJs) that render relatively high transendothelial electrical resistance (TEER). AD-associated breakdown of the BBB correlates with vascular Aβ deposition, suggesting that aggregated, pathological Aβ can modulate TEER. We explore leveraging this cellular response for early disease diagnosis via detection of early Aβ aggregates.

Primary human brain microvascular endothelial cells (HBMVECs) were cultured on a suspended membrane and supplemented to mimic the BBB. Once TEER values reflected TJ formation, HBMVEC monolayers were treated with oligomeric Aβ at picomolar to nanomolar concentrations, and TEER was monitored. Oligomeric Aβ at picomolar and nanomolar concentrations, but not monomer, induced a reduction of TEER and disruption of TJs. These results demonstrate that pathogenic Aβ oligomers are uniquely responsible for inducing endothelial monolayer permeability. By reducing monolayer electrical resistance, this response can be detected at physiological concentrations. This response was further explored with the influence of oxidative stress.

Cells were sensitized with low concentrations of hydrogen peroxide, and TEER was monitored following exposure to oligomeric Aβ. Inducing oxidative stress simultaneously with oligomeric Aβ treatment elicited a more pronounced decrease in TEER relative to oligomers alone. These results validate that introduction of physiologically active Aβ oligomers to a stress induced state can further decrease electrical resistance of an endothelial monolayer, while non-pathogenetic monomer remains inert.

Together, these results provide evidence that oligomers, the pathogenic form of Aβ, selectively break down the BBB. Translation of this experimental observation to a cell-based biosensor platform will lay the groundwork for the development of cost-effective, early AD detection.

Table of Contents

List of Figures

List of Abbreviations

Aβ.....amyloid-β protein

$A\beta_{1-40}$..... 40 amino acid isoform of amyloid-β protein

$A\beta_{1-42}$..... 42 amino acid isoform of amyloid-β protein

AC ..... alternating current

AD..... Alzheimer's disease

Ag.....silver

AgCl.....silver chloride

APP ..... amyloid precursor protein

BBB..... blood-brain barrier

BSA.....bovine serum albumin

CNS.....central nervous system

CSF ..... cerebrospinal fluid

CO_2.....carbon dioxide

DMSO ..... dimethyl sulfoxide

DLS.....dynamic light scattering

DPBS..... Dulbecco's phosphate buffered saline

ECGS .....endothelial growth serum

FPLC .....fast protein liquid chromatography

FBS .....fetal bovine serum

HBMVEC ..... human brain microvascular endothelial cell

HFIP..... 1,1,1,3,3,3-hexafluro-2-propanol

M ..... molar, SI unit for mol/L

NaCl ..... sodium chloride

NaOH ..... sodium hydroxide

NF-κB ..... nuclear factor-κB

PB ..... phosphate buffer solution

RT ..... room temperature

SEC ..... size exclusion chromatography

TEER..... transendothelial/epithelial electrical resistance.

TNFα ..... tumor necrosis factor-α

TNS ..... trypsin neutralizing solution

ZO-1 ..... zonula occludens

Chapter 1:

Introduction

1.1 Alzheimer's Disease

Alzheimer's disease (AD), a neurodegenerative disease characterized by progressive cognitive decline, ranks among the top 10 causes of death for Americans. AD accounts for about 80% of dementia cases in the US.[1] In South Carolina alone, the mortality rate from AD increased 165.8% from the year 2000. As our generations age, the prevalence of AD for our population will continue to grow. Evidence has shown that an earlier diagnosis leads to more effective treatment, in part because of the irreversible death of neurons. However, a cost-effective method for early diagnosis remains unavailable.

By the time a patient is presenting the earliest symptom of the disease, an estimated 20 years of brain changes have occurred.[2] The first manifestation of AD is also known as mild cognitive impairment (MCI).[3] Minor but noticeable decline in one's attention, learning and memory, executive function, processing speed, and semantic language characterize MCI.[4] Symptoms in AD progress further to one having difficulty remembering recent conversations, names, or events as well as feelings of depression and apathy.[1] Later in AD, symptoms include impaired communication, poor judgment, disorientation, confusion, as well as behavioral and personality changes. These symptoms can progress to difficulty in speaking, walking, and swallowing.[1]

AD pathogenesis relates to many complex pathways, including deficiency in cholinergic neurotransmission, tau protein deposition and phosphorylation, the involvement of inflammatory and oxidative pathways, and defective amyloid-β protein (Aβ) metabolism and deposition.[5] The cholinergic system is involved in the processes such as learning, memory, stress response, attention, wakefulness and sleep, and sensory information. Deficits in cholinergic transmission influence all aspects of cognition and behavior, including cortical and hippocampal processing information[6]. Other cholinergic deficits also alter the permeability of the BBB, hindering the elimination of amyloid plaques and further exacerbating the disease state.[7] Additionally, decreased levels of cytochrome c oxidase can cause dysfunction of mitochondria, and oxidative stress alters mitochondrial permeability. Mitochondria are the main contributors to reactive oxygen species (ROS) production which is greatly increased in AD.[8] Metal ions, specifically zinc and copper, can bind to Aβ plaques and produce ROS, bringing about oxidative changes and further lead to lipid and protein oxidation of the cell membrane. [7]

The deposition of aggregated Aβ plaques outside of neuronal cells and the accumulation of tau protein tangles inside the cell also characterize AD.[9] Soluble Aβ can also control the cleavage and phosphorylation of tau.[10] The excessive amounts of Aβ and neurofibrillary tangles, which are caused by hyper- phosphorylated tau,[3] is said to dysregulate the clearance mechanisms of the immune system. Immune cells are recruited to aid in clearance, however fail to effectively clear the protein which further increases pro- inflammatory cytokine and chemokine production.[11] Evidence of neuroinflammation results from clusters of microglia and astrocytes that have migrated to and surround Aβ plaques, in post mortem AD brains.[11] Specific regions of deposition

include the hippocampus, amygdala, entorhinal cortex, and basal forebrain, all of which influence memory, learning, and emotional behaviors.[9] Aggregated Aβ contributes to the damage and death of neurons by blocking communication at the synapse, impairing regular physiological activity,[12] and breaking down the blood-brain barrier (BBB).[9,13]

Risk factors for AD include age, family history, genetics, and general brain health and lifestyle choices. Most individuals with AD are 65 and older and the risk of AD doubles every 5 years.[1] People with a strong family history of AD are more likely to develop the disease. This can include both heredity and environmental factors such as inherited genetic mutations in APP, PSEN1, and PSEN2.[10] The common thread to all of these mutations is that they increase production and aggregation kinetics of $A\beta_{1-42}$.[10,14] Less than 1% of AD cases are caused by deterministic genes, which are genes that cause a disease, instead they increase the probability for developing AD. However, carrying the allele ε_4 of Apolipoprotein E (APOE- ε_4) has been recognized as the strongest risk factor for sporadic AD.[15,16] Apolipoprotein E (ApoE) isoforms also influence the clearance and deposition of Aβ. This protein is coded by the APOE gene which has 3 major alleles.[15] Other injuries, medical conditions, and environmental factors are linked as risks for AD. For example, a traumatic brain injury can accelerate Aβ production and accumulation. It is hypothesized that vascular damaged from TBI can trigger the AD pathology and is associated with cerebrovascular dysfunction.[17] Low mental status, low mental and physical activity, and low educational and occupational status correlate with AD. Furthermore, cardiovascular risk such as heart disease, diabetes, stroke, high blood pressure, high cholesterol, smoking, and obesity increase the risk of AD.[1,14,18]

Current clinical diagnostic tools require cognitive, functional, and behavioral tests after a patient has displayed progressive cognitive decline.[19] The presence of cognitive decline points to irreversible neuronal cell death. After clinical tests are preformed, imaging studies aid in diagnosis confirmation. Imaging studies consist of magnetic resonance imaging (MRI), but more often positron emission tomography (PET). PET can reflect resting state cerebral metabolic rates of glucose, which indicates neuronal activity. PET image tracers that correlate with Aβ deposition are used to probe for the presence of deposited Aβ plaques, a characteristic of AD.[3] However, a postmortem neuropathological examination is the gold standard for identifying if a patient had AD or any other form of dementia.[7,20]

Mixed pathologies contribute to inaccurate diagnoses and treatments, which highlights the importance of defining antemortem criteria for diagnosis. The development of therapeutics is limited by the ability to assess early disease progression. Earlier and more reliable diagnostics will allow for better assessment of disease progression and facilitate clinical trials of prospective therapies to combat the disease itself. The physiological consequences of AD call for a method to detect the disease before clinical symptoms arise.

1.2 Amyloid-β: Origin, Aggregation, and Toxicity

In 1991, Dr. John Hardy and Dr. David Allsop presented their discovery of a pathogenic mutation in the amyloid precursor protein (APP) gene located on chromosome 21. They described a pathological cascade in which the disease progresses in order of Aβ deposition, tau phosphorylation and tangle formation, resulting in neuronal

death.[21] Today, this phenomenon is widely accepted and referred to as the amyloid cascade hypothesis. [8]

Aβ is part of a family of amyloid proteins, which share the ability to form β- pleated amyloid sheets and become resistant to breakdown from enzymes.[22] $A\beta_{1-40}$ is the predominant form of the protein in the brain during physiological conditions, but $A\beta_{1-42}$ is the dominant type found in the plaques which are deposited on the brain in AD and characterized the disease.[16] Aβ monomer is a typical product of cellular metabolism resulting from proteolytic processing of APP.[23] APP is a type 1 transmembrane protein[16] with a large extracellular domain[10]. APP is synthesized in the endoplasmic reticulum, transported to the Golgi complex, and subsequently transported to the plasma membrane[23]. At the plasma membrane, APP processing happens in two alternative pathways, the amyloidogenic and non-amyloidogenic pathways.

In the non-amyloidogenic pathway, APP is cleaved by α-secretase producing a soluble N-terminal fragment, resulting in the soluble APP fragment (SAPPα) and membrane bound C-terminal fragment. The C-terminal fragment can further be cleaved by γ-secretases generating a soluble extracellular p3 peptide, which can be further degraded. The non-amyloidogenic pathways prevents the formation of intact Aβ.[24]

The amyloidogenic pathway involves sequential cleavages by β- and γ-secretase at the N- and C-termini, respectively, and the resulting forms are the 40 and 42 amino acids, $A\beta_{1-40}$ and $A\beta_{1-42}$.[23] $A\beta_{1-40}$ is the normal soluble isoform that comes from APP; however, if the cleavage pattern changes the isoform $A\beta_{1-42}$ is the result. The isoform of $A\beta_{1-42}$ has two additional amino acids, isoleucine and alanine. When the protein misfolds

to form the amyloid state, the backbone N-H and C=O groups are exposed, allowing the protein to hydrogen bond with other protein chains and form aggregates.[22] Additionally, the presence of aggregates can seed nucleation of monomers, a process that eliminates the lag time to nucleation observed for aggregation initiated with monomeric protein alone.[25,26] These conformational changes allow Aβ to more easily aggregate and deposit as insoluble plaques on and around the brain vasculature. Factors affecting the upregulation of the amyloidogenic pathway include age, traumatic brain injury (TBI), genetic factors, inflammation, and oxidative stress.[10]

1.3 The Blood-Brain Barrier

While the brain constitutes just 2% of body mass, it consumes over 20% of total body oxygen and energy.[27] The complexity of the central nervous system (CNS) requires high organization and stable biochemical conditions for proper function.[28] This function is maintained by an anatomical barrier, the blood-brain barrier (BBB), which separates blood and neural tissue.[29] The BBB describes the distinctive properties of the microvasculature of the CNS, and is a highly selective and dynamic interface between blood circulation and the CNS. The vessels of the BBB are continuous nonfenestrated vessels that contain unique properties that allow for the regulation of molecules, ions, and cells between the blood and the CNS.[30] The BBB simultaneously supplies oxygen and nutrients, allowing for CNS regulation to ensure homeostasis by tightly regulating the transport of nutrients, metabolites, and waste products between the blood and the brain. The restrictiveness of the barrier blocks the entry of neurotoxic molecules and protects the CNS from injury, diseases, toxins, and pathogens.[30]

Central to the BBB is a monolayer of highly specialized microvascular endothelial cells, which make the vessels and capillaries. These endothelial cells exhibit low permeability and junction proteins that render their barrier 50- to 100-fold tighter than peripheral capillaries.[31] Along the capillary walls of the BBB, a single layer of endothelial cells is closely connected by tight junction proteins that line the cellular borders.[30,32-34] Tight junctions involve occludin and claudin-1, -3, -5, and -12 and the membrane-associated guanylate kinase tight junction proteins ZO-1, -2, and -3.[13] These tight junction proteins are required for a healthy, intact monolayer that renders relatively high transendothelial electrical resistance (TEER).[30,32] The endothelial cells of the BBB exhibit higher volumes of mitochondria, which aid in their selective molecular permeability.[29] The polarity of endothelial cells is a key feature of the BBB; this polarity is necessary for the selective transcellular transport of solutes and regulatory function.[28,34,35] The endothelial cells of the BBB undergo meager rates of transcytosis compared to peripheral endothelial cells; however, in injury or disease, up-regulation of this transcytosis is often seen. [30] Surrounding pericytes, astrocytes, microglia, and neurons influence this endothelial layer. Together, these cells form the neurovascular unit (NVU).[29,34,36] The NVU maintains homeostasis across ~645 kilometers of capillaries in the brain via the cellular and extracellular influences on BBB function and cerebral blood flow. [37,38]

Endothelial dysfunction limits the properties of the BBB, leading to increased vascular permeability and an inability to maintain homeostasis.[28] A leaky BBB allows for the influx of toxic molecules, leading to impaired brain homeostasis, inflammation, and irregular neurovascular function.[14] Cerebrovascular dysfunction is one of the earliest

events in the pathogenesis of AD.[14] Studies have shown that the BBB becomes leaky in AD, allowing blood-borne molecules to enter the brain, triggering an inflammatory response. This inflammatory response can later lead to neuronal damage and cell death. This dysfunction further leads to breakdown of the BBB. This breakdown is characterized by: cellular deterioration of endothelial cells and pericytes[9]; tight and adherents junctions expression reduction; capillary basement membrane changes, and amplified bulk flow transcytosis.[13]

Cerebral amyloid angiopathy (CAA) describes the deposition of amyloid around the brain vasculature. 90% of patients with AD also have CAA.[14] Aggregated Aβ protein deposition around the brain vasculature is a prominent characteristic of AD and results in BBB breakdown. Both CAA and AD pathologies are driven by impaired Aβ clearance resulting in increased vascular deposition of Aβ.[39] While these two conditions often overlap, the mechanisms that lead to brain injury are not the same. CAA is vascular brain injury and AD is neurodegenerative brain injury;[39] however, BBB dysfunction has been identified in both disease pathogenesis. The presence of CAA in AD is associated with greater cognitive impairment, and faster more pronounced cognitive decline.[39]

Studies have suggested that Aβ can disrupt the BBB and contribute to the pathogenesis of AD. Aβ can induce oxidative stress and inflammation in the endothelial cells that form the BBB, leading to dysfunction and damage to the barrier.[13] Aβ can activate matrix metalloproteinases, enzymes that degrade the extracellular matrix of the BBB, and increase the permeability of the barrier. Aβ can interact with the receptor for advanced glycation end-products (RAGE) on the surface of the endothelial cells and activate downstream signaling pathways that promote BBB disruption.[40] These findings

indicate that Aβ-induced BBB dysfunction may contribute to the disease progression of AD and highlight the importance of maintaining a healthy BBB for both preventing and treating AD.

A common method to investigate the BBB is the use of *in vitro* models that simulate the interactions of endothelial cells and other components of the BBB. One commonly used *in vitro* cellular model is one that employs a semipermeable suspended system. This format is common due to ease of use, adaptability to multicellular models, flexibility in cellular arrangement, and low cost.[41] The semipermeable membrane used in these culture models ranges in pore size (0.4 to 8.0 μm) and material (polycarbonate, polyester, polytetrafluoroethylene).[42] To increase cell attachment, some models incorporate coatings to mimic the basement membrane, facilitate attachment, and provide structural support. These coatings involve single proteins or standard protein mixtures. Cells can be cultured alone on the apical surface of the membrane. Additional cell types may be added on the basolateral surface of the membrane, where they initiate polarization, as well as on the bottom surface of the basolateral well chamber and/or suspended within the apical or basolateral chamber, where they introduce non-contact cell influence. Agents can be administered to the apical or basolateral side of the barrier.

1.4 Innovation

AD starts 20 years before symptoms arise, and as insoluble fibrils form and deposit on the brain the levels of Aβ in cerebrospinal fluid (CSF) decline compared to when no plaques are present.[43,44] In early stages of AD the concentration of $A\beta_{1-42}$ in the CSF starts to decrease while concentrations in the brain increase,[9,49] suggesting diminished transport of Aβ from the brain.[10] These results allude that the optimal time to

test for the presence of Aβ oligomers in a patient's CSF is prior to symptoms, because of a higher concentration of Aβ in CSF.

Smaller soluble aggregates, specifically oligomers, are the most neurotoxic form of the protein and are thought to lead the progression of the disease.[10,12] Aβ oligomers have been shown to selectively disrupt calcium release in neuronal cells leading to synaptic dysfunction,[45] and induce significant inflammatory responses in endothelial cells.[46] Prior results revealed that incubating rat brain microvascular endothelial cells with small aggregates of $A\beta_{1\text{-}40}$ induces endoplasmic reticulum stress leading to the apoptotic cell death pathway. [47] Further, Aβ aggregates induce permeability of human brain microvascular endothelial (HBMVEC) cells, with the most pronounced effects elicited by the smallest aggregates. The small aggregates cause tight junction protein breakdown and recruitment away from cell boarders.[48] Evidence has been provided that these Aβ aggregates activate NF-κB in HBMVECs[49] and iPSC derived endothelial cells.[46] Aβ aggregates induce a phenotypic change in HBMVECs as well as increased monolayer permeability and monocyte infiltration.[49] These findings further confirm that Aβ aggregates lead to vascular alternations and a deteriorated BBB.

While these results seen in the literature confirm the toxicity of small Aβ aggregates, there is a lack of data in the physiological concentrations on the brain endothelium. In this study, we explore if vascular breakdown can be observed at concentrations closer to the concentrations found *in vivo* prior to symptoms arising. We also explore if we can detect these vascular changes electrically. Subsequent research provides evidence that physiological relevant concentrations of Aβ oligomers can be

detected utilizing a method that could be translated to a sensing platform for early detection.

1.5 Study Overview

The goal of this work was to infer if there is a method to detect physiological Aβ oligomers that can be translated to a platform that can be rendered for early disease detection. To do so, we first develop an *in vitro* human cellular model of the BBB, which renders a relatively high electrical output. Next, this BBB model is applied to investigate the effects of different forms of the protein Aβ and its effects on cellular electrical resistance. To further exacerbated the disease state, oxidative stress was induced by sensitizing the model with a common ROS, hydrogen peroxide (H_2O_2). We explored the effect of physiological ranges of Aβ on cells in a stressed oxidative state. This sensitization also allows for a more pronounced electrical response reducing the limits of detection. These studies entail three aims of research, which are reviewed below.

1.5.1 Characterize, develop, and implement a cellular in vitro model representative of the blood-brain barrier.

To effectively study the effect of Aβ, we must begin our assessment with an in vitro model that is representative of the BBB. Transendothelial electrical resistance (TEER) is a rapid, noninvasive approach to probe endothelial cell monolayer permeability.[50] A high resistance measurement indicates a strong, healthy monolayer, while a decrease in resistance points to monolayer disruption.[51] The characteristics of the BBB render a relatively high TEER. The goal of this aim is to achieve a cellular model representative of the BBB in which TEER can be evaluated. Cell seeding density,

membrane type, ECM membrane coatings, and medium additives were evaluated and combined to achieve a superior model.

1.5.2 Characterize the endothelial monolayer response to Alzheimer's disease associated-Aβ

Many studies have explored the endothelial response to oligomeric Aβ, however the cellular electrical response to physiological concentrations has not been thoroughly explored. To quantify an electrical response to the Alzheimer's associated form of Aβ cells were treated with the protein and the response was evaluated. In this study, the electrical response of endothelial cells in the presence of oligomeric Aβ was investigated.

1.5.3 Explore a mode in which exacerbates the effects of toxic Aβ on the model.

To yield a more pronounced response to physiological concentrations of Aβ oligomers, two methods were explored. The first method utilized the know nucleation dependent nature of aggregation. Samples were co-incubated with monomeric Aβ to investigate if further nucleation would produce more small aggregates and increase the cell response. Second, sensitizing cells with low concentration of H_2O_2 were tested to stimulate oxidative stressed and explore if sensitization would induce a more pronounced response.

Chapter 2:

Materials and Methods

2.1 Materials

Lyophilized crude $A\beta_{1-40}$ was purchased from Peptide2.0 (Chantilly, VA). $A\beta_{1-42}$ was obtained from AnaSpec, Inc. (San Jose, CA). Dimethyl sulfoxide (DMSO) was purchased from EMD Biosciences (San Diego, CA). Bovine serum albumin (BSA), bovine plasma fibronectin, was purchased from ScienCell Online (Carlsbad, CA). Hydrocortisone and hydrogen peroxide was purchased from Sigma-Aldrich (St. Louis, MO). Transwell permeable supports were purchased from Corning (Lowell, MA). Nitrocellulose membranes, Lamielli buffer, Western C standard, horseradish peroxidase and anti-amyloid-β 6E10 primary antibody, anti-β amyloid primary antibody was purchase from BioLegend (San Deigo, CA). Secondary antibody was purchased Rockland Chemical (Pottstown, Pa). Collagen type I was purchased from Advanced Biomatrix, Inc. (Carlsbad, CA). Gelatin solution-type B, 2% in H_2O and hydrocortisone was purchased from Sigma-Aldrich (Saint Louis, MO). BD Matrigel basement membrane matrix was acquired from BD Biosciences (San Jose, CA). ThinCert culture cup inserts were purchased from Greiner Bio-One (Monroe, NC). Bovine Plasma Fibronectin and fetal bovine serum (FBS) was purchased from ScienCell Online (Carlsbad, CA). Erythrosin blue was purchased from the University of South Carolina School of Medicine (Columbia, SC).

2.2 Cell culture

Primary human brain microvascular endothelial cells (HBMVECs) were purchased from ScienCell online at passage 1, expanded and persevered at passage 4 in cell freezing media purchased from ScienCell online, and stored in liquid nitrogen vapor until experimentation. Cell cultures were maintained in a T75 Delta Nuclon EasYflask purchased from ThermoFisher Scientific (Waltham, MA) coated with 12 µg/mL bovine plasma fibronectin at 37 °C in a humid atmosphere of 5%/CO2 /95% air. Cells were maintained in complete classic medium, purchased from ScienCell Online (Carlsbad, CA). Complete classic medium kit consisted of endothelial growth serum (ECGS), 100 units/mL penicillin, 100 µg/mL streptomycin, and 5% FBS.

2.3 Oligomer preparation

Synthetic $A\beta_{1-42}$ was reconstituted in cold 1,1,1,3,3,3-hexafluro-2-propanol (HFIP) to a concentration of 4 mg/mL and incubated on ice for 60 minutes. After incubation Aβ1-42 was aliquoted and left uncovered overnight at RT to allow HFIP to evaporate, resulting in a protein film. Protein films were stored at -80 °C until use. For experiments, fresh oligomers were prepared by reconstituting the protein films with dimethyl sulfoxide (DMSO) to a concentration of 1.5 mM and then further diluting to the concentration of 15µM with 12 mM phosphate buffer (pH 7.4) containing 1 µM NaCl to initiate oligomerization. After incubating for 30 minutes at RT oligomers were further diluted for use.

2.4 Monomer preparation

Lyophilized crude $A\beta_{1-40}$ was stored at -20 °C until reconstitution and preparation for experiments. To remove preexisting aggregates or seeds in which aggregates can

grow, $A\beta_{1-40}$ was purified using fast protein liquid chromatography (FPLC) that utilizes size exclusion chromatography (SEC) on a Superdex 75 HR10/30 column (GE Healthcare, Piscataway, NJ). Aβ dissolved in 50mM NaOH and at concentrations around 2mg/mL. The column was pretreated with 2 mg/mL of bovine serum albumin (BSA) to reduce nonspecific Aβ interaction with the matrix of the column. The protein eluted in a 12 mM phosphate buffer solution (pH 7.4). The concentrations of isolated monomer were determined by measuring the UV absorbance from a 200-400 nm wavelength scan. Samples were further diluted to needed concentrations and immediately used for experiments.

2.5 Western blotting

For confirmation of the presence of oligomeric Aβ, get electrophoresis and western blotting techniques were used. Samples were mixed with in a 1:1 ratio with Laemilli Buffer. Gel electrophoresis was first used to separate the protein by molecular weight. The proteins were run at 120 V on the gel until the dye reached the bottom of the gel. Proteins were then transferred from the gel to nitrocellulose transfer membrane using semi-dry transfer run at 14 V for 15 min. The transfer membrane was then blocked overnight with a blocking buffer. Aβ was detected with the 6E10 antibody, and proteins were detected by visualizing chemiluminescence on a iBright Imaging System (Thermofischer Scientific, Waltham, MA).

2.6 Transendothelial electrical resistance measurements

TEER, which reflects the resistance to ion diffusion across a cell monolayer was measured once a day, 24 h post-seeding, in a laminar flow hood at RT. Measurements were acquired using an Endohm chamber (World Precision Instruments, Sarasota, FL),

wherein a pair of concentric electrodes incorporating a voltage-sensing Ag/AgCl pellet in the center and an annular current electrode are positioned on both sides of the cells grown on a semipermeable membrane.[52] The suspended membrane is placed in the EndOhm chamber and an ±10 μA square wave alternating current (AC), and a 12.5 Hz signal is applied to the monolayer using and epithelial voltohmmeter (EVOM2) (World Precision Instruments, Sarasota, FL). The electrodes measure both the current and voltage across the cell layer, and output as a the total resistance (R_{total}).[50,53]

R_{total} is a sum of the transcellular resistance ($R_{transcellular}$= R_{t1} + R_{t2}) and paracellular resistance ($R_{paracellular}$ = R_{p1} + R_{p2}) in parallel (Figure 2.1). To obtain resistance of the monolayer (R_{cells}) the background resistance was taken using a transwell absent of cells with the selected coating (R_{insert}), and then subtracting the background resistance from the (R_{total}). For true tissue resistance in $\Omega \cdot cm^2$ the resistance measurement was multiplied by the area (A) of the semipermeable membrane (0.336 cm^2).

$$\frac{1}{R_{total}} = \frac{1}{R_{Transcellular}} + \frac{1}{R_{Paracellular}} \quad \text{Equation 2.1}$$

$$R_{cells} = R_{total} - R_{insert} \quad \text{Equation 2.2}$$

$$TEER\ (\Omega cm^2) = R_{cells} \times A \quad \text{Equation 2.3}$$

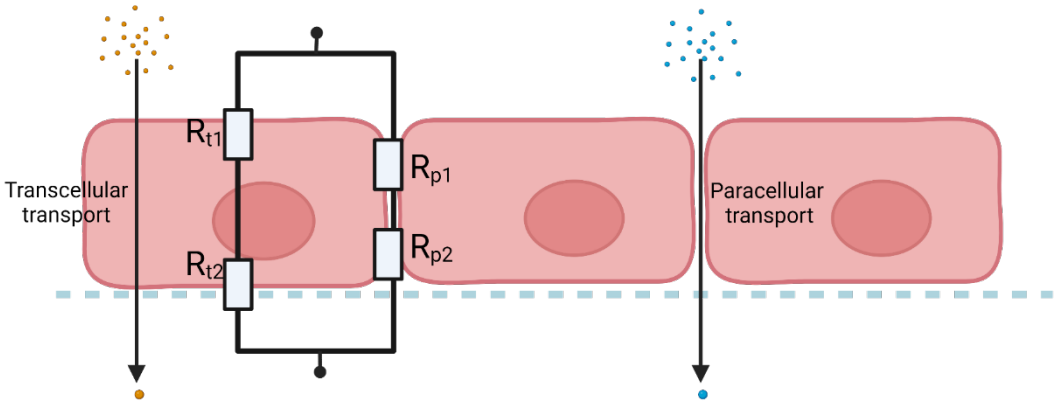

Figure 2.1 Transendothelial electrical resistance. Equivalent circuit model of a cellular monolayer consisting of a transcellular transport route and a paracellular transport route for current passing through the membrane. Created with BioRender.com

Chapter 3:

Development and Characterization of *In Vitro* BBB Model

3.1 Introduction

To effectively study the influence of Aβ on the BBB, an accurate *in vitro* model is needed. This chapter describes the development of an *in vitro* BBB model in which will be utilized to further understand the impact of Aβ on the electrical resistance of the BBB. The goal of this work was to render a model in which TEER could be evaluated. TEER is a non-invasive was to probe an endothelial or epithelial cellular monolayer.[50,54] As cells grow and form tight junctions, the electrical resistance across the monolayer increases reflecting the tightness of the barrier. TEER values have commonly been used to assess the effects of drugs, toxins, and other interventions on the endothelial barrier *in* vitro, and to study the mechanisms of barrier function and dysfunction in various diseases and conditions. To render an accurate BBB model to measure the electrical resistance of cells, multiple coatings, membranes, and pore sizes were explored. Much trial and error came with establishing this model; however, an optimal *in vitro* cellular model was achieved. The resulting protocol established from this study was what subsequent research was pursued.

3.2 Materials and Methods

3.2.1 Cell seeding protocol

Cells were maintained as described Section 2.2. For seeding on the suspended membrane, cells were first rinsed with RT Dulbecco's phosphate buffered saline (DPBS). A 0.01% trypsin/EDTA (T/E solution) solution was added to the flask and cells were monitored under the microscope. Once the cells rounded the T/E solution was transferred to a 50 mL conical tube containing 5 mL of FBS. The flask was then incubated for 1 min at RT and 5 mL of trypsin neutralizing solution was transferred to the flask twice to dislodge any remaining cells. The TNS was then transferred to the 50 mL conical tube containing FBS and centrifuged for 5 min at 1000 rpm. The resulting cell pellet was resuspended in complete classic medium containing 550 nM hydrocortisone. 40 µL of cell stock was diluted 1:5 with erythrosine blue to assess cell viability and loaded into a hemacytometer to determine cell density.

3.2.2 Membrane coating

For gelatin coating, the gelatin solution was allowed to liquefy in the 37°C. Transwells were coated with 20 µL of gelatin solution at concentration 0.4 mg/cm^2. Transwells were allowed to dry for at least 2 h at RT. For the gelatin and collagen type 1 mixture, gelatin was warmed as mentioned above, then collagen was mixed into the gelatin solution for a final concentration of 100 µg/mL collagen and 0.4 mg/cm^2 gelatin. Matrigel coating was applied using the thin gel method. Using cooled pipets, the Matrigel was mixed to homogeneity. The transwell plates were kept on ice and 50 µL/cm^2 of solution was administered to the transwells. Plates were incubated at 37 °C for 30

minutes. After incubation, excess unbound material was aspirated, and cells were seeded on the transwell. Fibronectin was diluted to 12µg/mL concentration and administered to wells at room temperature and incubated at 37°C for 2 h. After incubation, excess unbound material was removed, and the cells were seeded on transwells.

3.3 Results and Discussion

Using TEER provides a precise and sensitive method for studying the dynamics of the BBB and its functional role in AD. To accurately study AD, a model representative of the BBB must first be achieved. Only endothelial cells were implemented into the model for experimental feasibility. While some BBB models incorporate multiple cells times to be more representative of the NVU, the intention of this project is to ultimately translate experimental findings to a biosensing platform. Culturing just endothelial cells allows for reduced complexity, which when increased also increases model failure. Endothelial cells solely comprise the BBB; therefore, biological relevance is achieved with just this cell type.

Primary cells were chosen for this model due to the physiological relevance. These primary cells are derived directly from the capillaries of the brain, making them more representative of the *in vivo* environment. Primary cells have a finite life span, and when outside of their native environment, they lose their unique protein expression pattern and display a more generic endothelial cell phenotype.[55] Knowing this, low passages were chosen for experimentation and media supplementation was employed. Cells were used for experimentation between passage 6 and 10. Both polycarbonate (PC) and poly(ethylene terephthalate) (PET) membranes were compared for cell growth. Cells

grown on PET membranes displayed minimal barrier properties via low TEER measurements relative to the PC membranes; therefore, a PC membrane type was chosen.

Pore sizes of 0.4, 3.0, and 8.0 μm were compared within the PC membrane type. The membranes with 8.0 μm pores showed the most prolific growth and were therefore continued with throughout experiments. HBMVECs were seeded at different densities ranging from 5,000 to 100,000 cells/well to determine which density rendered the highest electrical resistance. The monolayer was more consistent with a seeding density of 50,000 cells/well.

The seeding density of 50,000 cells/well were seeded onto PC membrane coated with either fibronectin, Matrigel, Attachment Factor, or a gelatin: collagen mixture. TEER was acquired each day after seeding. Results indicated that Matrigel coating did not harbor cell growth. When cells were seeded onto Matrigel coated PC membranes TEER values reflected a minimal increase. Cell culture medium of these cells was observed to be cloudy. From this observation, further TEER measurements were not acquired on this coating, and further testing was relinquished. Collagen: gelatin and Attachment Factor coatings show enhanced cell growth, but these coatings were relatively unstable increasing and decreasing TEER over time. Instead of increasing TEER and plateauing after increased growth, indicating a mature and stable monolayer, the collagen: gelatin and Attachment Factor coatings displayed inconsistent barrier properties reflected by fluctuations in TEER values. The fibronectin coated membranes showed the most uniform barrier integrity which was reflected by a steady increase in TEER values. The fibronectin coating was ultimately chosen for final optimization (Figure 3.1).

To combat the phenotypic loss of expression of primary cells outside of their native environment, hydrocortisone was used to enhance barrier properties.[56] Hydrocortisone is a glucocorticoid and influences the metabolism of many cells and can improved the TEER of endothelial monolayers.[57] By reducing the FBS content of the cells and maintaining the hydrocortisone concentration the monolayers exhibited a higher TEER value and a normal cell growth curve. This response was best enhanced after reducing FBS content in the medium to 1% after 3 days post-seeding on the transwell membranes when compared to reducing FBS content 2 days post-seeding (Figure 3.2). Further observations concluded that when the membranes were wetted with medium before seeding, more uniform cell growth was observed between induvial wells. Therefore, each well was wetted for at least 30 min prior to cell seeding.

The optimal and most consistent barrier properties were seen by employing the following final protocol. Cells were only used between passage 6 and 10. Transwells were coated with 12 µg/mL of bovine plasma fibronectin and incubated for at least 2 h, but up to 24 h at 37°C in a humid atmosphere of atmosphere of 5%/CO2 /95% air. After incubation, fibronectin was aspirated, and wells were wetted with 250 µL in the apical chamber and 1mL in the basolateral chamber of complete classic medium containing 550 nM hydrocortisone at 37°C in a humid atmosphere of 5% CO2/95% air. After incubation of at least 30 min, apical medium was removed, and cells were seeded at a density of 50,000 cells/well. One day post-seeding, basolateral medium was replaced with fresh medium. Following media changes occurred in both the apical and basolateral chamber every 24-48 h. Three days post-seeding, medium was switched to one containing 1% FBS, 550 nM hydrocortisone, 100 units/mL penicillin, and 100 µg/mL streptomycin.

Once TEER values plateaued indicating monolayer confluence, cells were used for experiments.

TEER measurements allow for understanding the functional effects on HBMVECs when exposed to toxic aggregates, but also have potential to be used as an accurate diagnostic tool. By incorporating TEER measurements with the *in vitro cellular* BBB model established in this chapter, we can investigate the electrical impact of Aβ on the BBB.

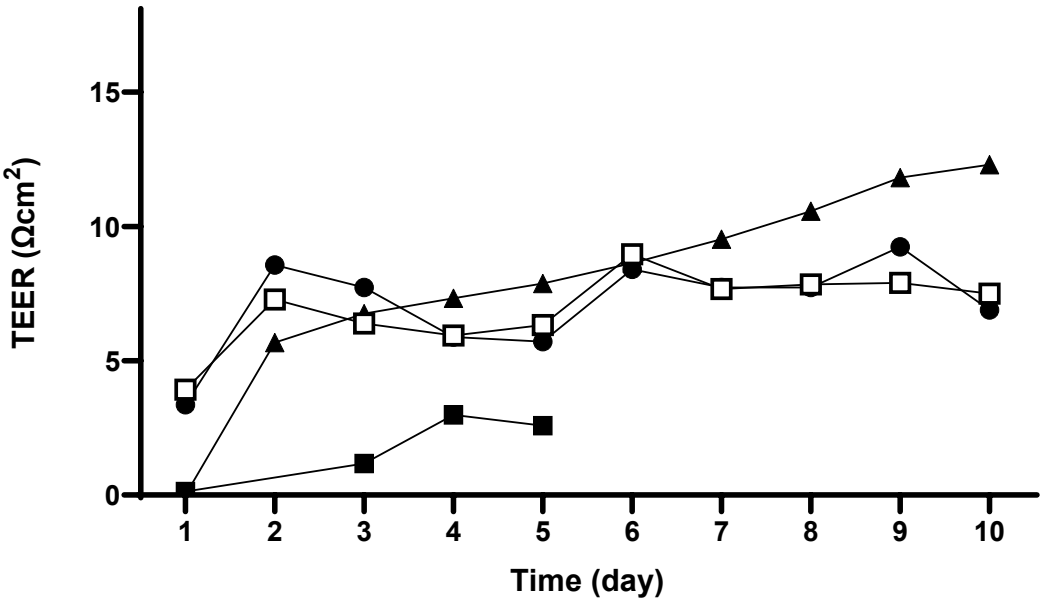

Figure 3.1 Membrane coatings support varying cell growth. HBMVECs were seeded with 50,000 cells/well on PC transwells with 8.0 μm pores with coating of gelatin:collagen (□), Attachment Factor (●), fibronectin (▲), and Matrigel (■). TEER was measured every 24 h after seeding. Each point represents an average of 10-12 wells.

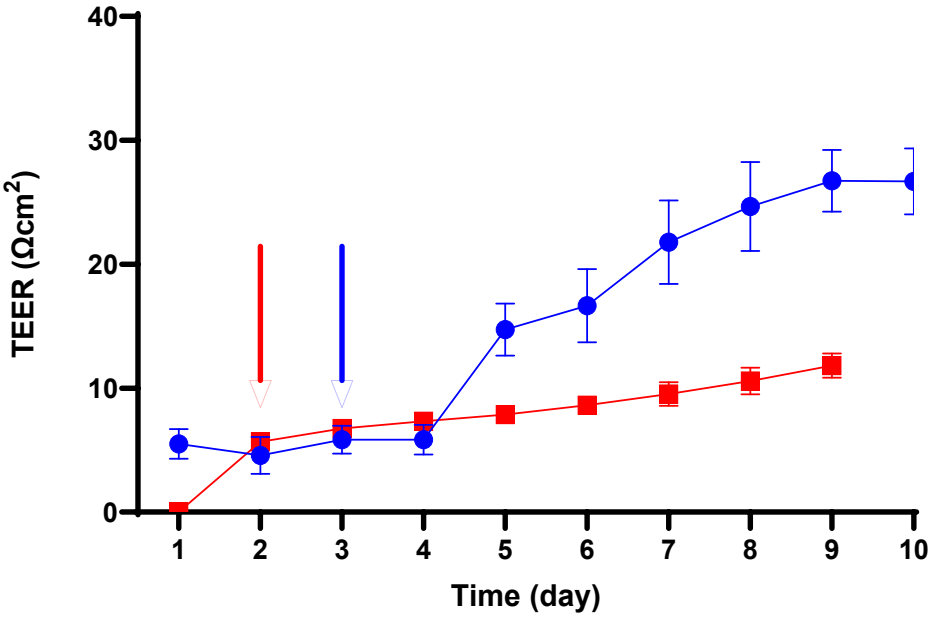

Figure 3.2 Time at which FBS content is reduced influences TEER. Reducing the FBS content 3 days after seeding cells (●), resulted in increased TEER and cell growth when compared to reducing FBS 2 days after seeding (■).

Chapter 4:

Endothelial Monolayer Response to Aβ

4.1 Introduction

During normal aging, some BBB breakdown transpires in the hippocampus; however, this breakdown is more prominent in MCI compared to age-matched neurologically healthy control patients.[58] This pronounced breakdown may precede the hippocampal atrophy that is seen later in AD. Studies have shown that small soluble aggregates have toxic effects on multiple mechanisms involving the brain and the BBB. More specifically, they show the activation of apoptotic pathways, oxidative stress, cellular membrane alterations, and vascular breakdown.[20,39,59] The physiological plasma concentration of $A\beta_{1-42}$ found in amyloid PET positive patients is averaged at ~9.3 ρM and 7.5 ρM for amyloid negative patients, and the concentrations found in CSF are approximately 4 times higher.[43] While prior results confirm the toxicity of soluble Aβ aggregates to both neuronal and endothelial cells, the concentrations which are often tested are magnitudes larger than anything found physiologically.[47-49]

Previously in our laboratory, HBMVEC monolayers were exposed to $A\beta_{1-40}$ aggregates mixtures ranging in a variety of average aggregate size. It was found that the smallest average sized aggregates had the most pronounced effects on the HBMVEC monolayers. Changes in monolayer permeability, tight junction re-localization, and TEER reduction was more pronounced for the smallest aggregates.[48] Since the smallest

sized aggregates have been deemed to be the most potent on HBMVECs, we chose to specifically investigate the oligomeric size of aggregates.

To do so, we oligomerize $A\beta_{1-42}$ and treat the *in vitro* cellular model established in Chapter 3 with oligomers. To confirm the presence of oligomers in samples, dynamic light scattering (DLS) and western blotting were employed prior to experiments. Further, the confirmed oligomers were added to established HBMVEC monolayers. To investigate the threshold in which cells produce a response, cells were treated at a range of concentrations. This chapter identifies and characterizes the form of Aβ that induces a change in endothelial monolayer electrical resistance and a threshold in which that response can be determined.

4.2 Materials and Methods

4.2.1 Oligomer preparation

Oligomers were prepared as detailed in Section 2.3. After the 30-minute oligomerization, the reaction was halted by diluting with 1% FBS, 550nM HC endothelial cell medium. For confirmation of oligomers, the freshly prepared oligomers were used at the 15 μM concentration. Oligomers were serial diluted to concentrations ranging from 1 ρM to 1000 nM. For cell treatments, immediately after dilution, Aβ oligomers were administered apical chamber of the suspended membrane (Figure 4.1).

4.2.2 Dynamic light scattering

The Aβ size and polydispersity index were measured using a Zetasizer Nano ZS system (Malvern Instruments Ltd., Worcestershire, UK). Measurements were made at room temperature and samples (15μM) were placed in a disposable cuvette and light

scatter intensity was collected using a 60 s acquisition time. Intensity fluctuations generated by the velocity of the Brownian motion yield the particle size and the hydrodynamic radius (R_H) can be determined using the Stokes-Einstein relationship. 3 acquisitions per sample were averaged for each experimental run, and a histogram of percentage of sample vs R_H was analyzed using excel.

4.2.3 Western blotting

Freshly prepared oligomers at a 15 μM concentration were analyzed using western blotting as detailed in Section 2.5

4.2.4 Cell culture

To explore the effect of Aβ on endothelial monolayers, HBMVECs were used. Cells were maintained and seeded in the optimized protocol described in Chapter 3.

4.2.5 Transendothelial electrical resistance

To monitor the effect of Aβ on HBMVEC monolayers, TEER measurements were used. The measurements were obtained as described in Section 2.6. Results are reported in fraction of TEER retained, wherein the TEER value of an individual well after treatment is divided by the value of the well prior to treatment.

$$Fraction\ of\ TEER\ retained = \frac{TEER_{post-treatment}}{TEER_{pre-treatment}} \qquad \text{Equation 4.1}$$

4.2.6 Statistical analysis

GraphPad Prism 9.0 software was used to analyze data obtained from oligomeric Aβ treatments. Generated data for each concentration was analyzed for statistical

significance via one-way ANOVA with multiple comparisons wherein each concentration was compared to the vehicle.

4.3 Results

4.3.1 Characterization of Aβ oligomers

The size and distribution profile of freshly prepared Aβ oligomers at a concentration of 15 μM were evaluated using DLS. This is the concentration in which the oligomerization reaction takes place, and samples are immediately diluted from. The polydispersity of samples is shown to have a range of hydrodynamic radii (R_H) from 27.6 and 39.41 nm to 229.35 nm (Figure 4.2). Measurements were run in triplicate and values are reported as an average of the sample. Of this entire sample, 99.9% of the sample R_H values fell within the range indicated above confirming the presence of the oligomers.

To again confirm the presence of Aβ oligomers, freshly prepared oligomers were separated using gel electrophoresis and western blotting techniques (Figure 4.2B). The presence of monomer, dimer, trimer, are all seen at their respective locations as well as higher molecular weight oligomers, which can be seen in the smear from 37 to 250 kDA.

4.3.2 Increased exposure to Aβ oligomers induces a more pronounced response in HBMVECs

Confluent HBMVECs were treated with Aβ oligomers and resistance measurements were procured 24 and 48 h after (Figure 4.3). The change in resistance was more pronounced in the 1, 100, and 1000 nM treatment and increased in the 10 and 30 nM treatment. Due to a greater resistance change in a larger percent and AD being a

chronic disease, the 48-h time point was chosen to be the reporting time. After 48 h, the untreated cells remained steady.

4.3.3 Aβ oligomers decrease TEER of HBMVECs while monomer remains inert.

Confluent HBMVECs treated with $A\beta_{1-42}$ oligomers at the concentrations of 1, 10, 30, 100, and 1000 nM all show a decrease in fraction of TEER retained. TEER measurements of the Aβ oligomer treated monolayers all decreased when compared to their measurements 48 h prior to treatment, indicated by a fraction of TEER retained value of lower than 1 (Figure 4.4). In contrast, confluent HBMVEC monolayers treated with $A\beta_{1-40}$ monomer isolated by SEC at concentrations of 0, 1, 10, 30, 2000 nM showed no resistance decrease (Figure 4.4). These results demonstrate that Aβ oligomers do affect the electrical resistance of HBMVEC monolayers while Aβ monomer remains inert.

4.3.4 Physiological concentrations can induce a significant decrease in TEER.

To explore if Aβ oligomers can induce the same response at physiological concentrations, confluent HBMVECs were treated with $A\beta_{1-42}$ oligomers at 1, 10, 100, and 1000 ρM for 48 h. A positive control of TNF-α at 20 units/mL was also applied to monolayers. The 1, 10, 100, and 1000 pM concentrations and positive control had retained 93.9, 92.9, 91.0, 91.1, and 80.6%, respectively (Figure 4.5). These treatments all significantly decrease TEER, indicating barrier breakdown. TEER remains steady in the presence of the negative control (0 pM) and reduces following treatment with oligomers of physiological concentrations and positive control.

4.4 Discussion

The $A\beta_{1-42}$ isoform is the predominant isoform aggregate in the amyloidogenic state, and its higher presence in the deposited amyloid plaques on the brain.[23,60] The toxicity of soluble Aβ aggregates have been reported to disrupt and alter the function of multiple mechanisms physiologically. The cellular response to Aβ has been explored in multiple facets on the different cells that comprise the NVU. Aβ oligomers have been identified to selectively disrupt mouse cortical neuronal calcium release[45] and endothelial mitochondrial function.[14] In the rat brain endothelial cell line RBE4, $A\beta_{1-40}$ aggregates has been shown to trigger apoptotic pathways by activation of the endoplasmic reticulum when exposed to 2.5 μM of $A\beta_{1-40}$.[47] This endothelial response was seen in both a dose and time dependent manner for the endoplasmic reticulum stress. Another murine model, utilizing the cell line bEnd.3, exposed to $A\beta_{1-42}$ oligomers revealed modest TEER disruption, intracellular oxidative stress, and reduced expression levels of tight junction proteins. Like the previous study, this effect was only seen at relatively high concentrations of Aβ oligomers, 10-40 μM.[61] Furthermore, $A\beta_{1-40}$ soluble aggregates at micromolar concentrations have induced permeability in HBMVECs and relocalized the tight junction-associated protein ZO-1. Relocation of ZO-1 away from the cellar borders into the cytoplasm indicates a decrease in barrier properties of the HBMVEC monolayer, which was confirmed to increased paracellular permeability.[48] Soluble aggregate mixtures of $A\beta_{1-40}$ initiated NF-κB signaling of HBMVECs.[49] Similarly, this upregulation of NF-κB signaling as well as TNF-α, IL-6, Casp3, SOD2, and TP53 has been reported to occur in iPSC derived brain microvascular endothelial cells exposed to $A\beta_{1-42}$ oligomers.[46] The NF-κB signaling pathway connects pathogenic signals and cellular danger signals to initiate cellular resistance to invading pathogens, and its

activation indicates an inflammatory response.[62] Some have hypothesized that Aβ inserts into the plasma membrane and creates a pore in the membrane which could be affecting TEER. A previous study has reported that $A\beta_{1-42}$ oligomers can accumulate in the lipid bilayer of the neuronal cell membrane. This study reveals that membrane Aβ accumulation and disruption arises from the hydrophilic residues located on the edges of the β-sheet structure, leading to the formation of lipid-stabilized pores. These pores therefore increase the transmembrane influx of ions through the cell.[63] While these results are shown in neuronal cells, the increase of ionic flow through the HBMVEC membrane could also cause a reduction in TEER. However, in this experimental system, Aβ is only administered apically so membrane insertion would possibly happen on the apical surface of the polarized HBMVECs.

There are multiple potential mechanisms by which Aβ is causing the reduction of TEER observed. Aβ oligomers could be affecting the resistance of the HBMVECs through mechanisms in which affect the cellular membrane. Increasing transmembrane pores by Aβ insertion would the ionic flow through the cells therefore decreasing the resistance of the HBMVECs. However, Aβ is only administered apically so this mechanism would only happen on the apical surface of the cells. Additionally, the loss of resistance could also be partially due to recruitment of tight junction proteins to the cell's nucleus lowering barrier properties, as also reported in the literature. It is proposed that not one specific mechanism is reducing this TEER reduction, but a combination of multiple mechanisms is compromised by the toxicity of Aβ oligomers increasing both paracellular permeability and transmembrane ionic flux.

This study has confirmed the presence of Aβ oligomers and its polydispersity by DLS and Western blotting. This work demonstrates that Aβ oligomers reduce the electrical resistance of HBMVEC monolayers, with a more pronounced response after 48 h treatments. Subsequently, this response can be seen in picomolar concentrations, which are relative to physiological levels. This work also validates that monomer remains inert to HBMVEC monolayers at the same treatment times. While multiple studies have shown the effect of Aβ oligomers on the endothelium, most concentrations explored were much larger than physiological levels. This work reveals that even low concentrations (nM and pM) can induce a response in cells. However, to employ this response for a more method of Aβ aggregate detection, a more pronounced response is preferred.

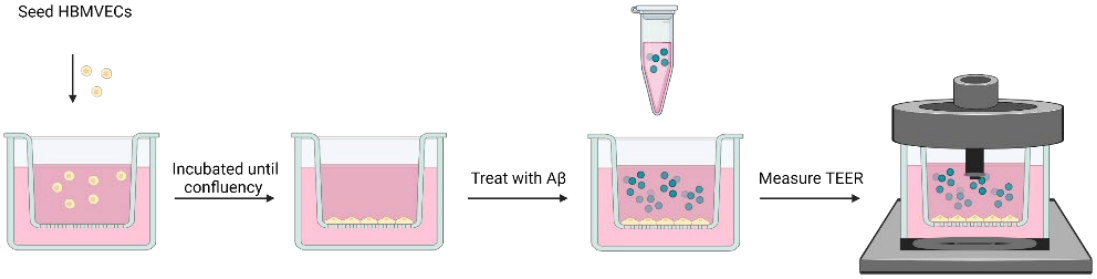

Figure 4.1 Aβ treatments of HBMVECs. HBMVECs were cultured on a suspended membrane to mimic the BBB. Once the monolayers reached confluence, confirmed by a plateau in TEER, they were treated with Aβ oligomers or monomer. Created with BioRender.com

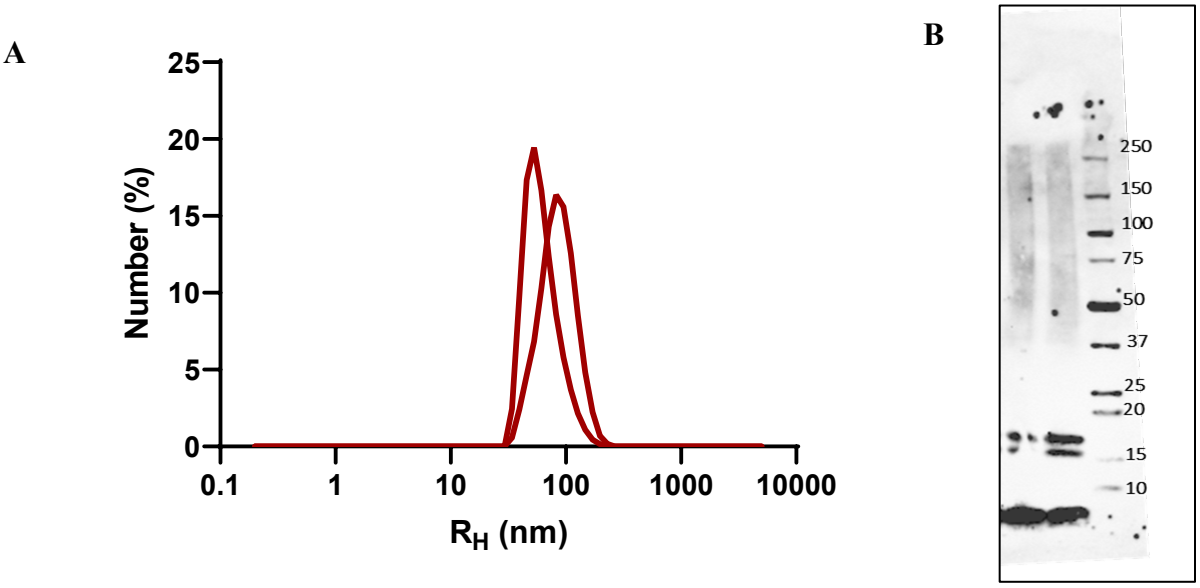

Figure 4.2 Characterization of oligomers. $A\beta_{1\text{-}42}$ oligomers (15 uM) were prepared via a 30-min oligomerization with 1μM NaCl in 12 mM phosphate buffer. Protein size was assessed via hydrodynamic radius (A) and western blotting (B).

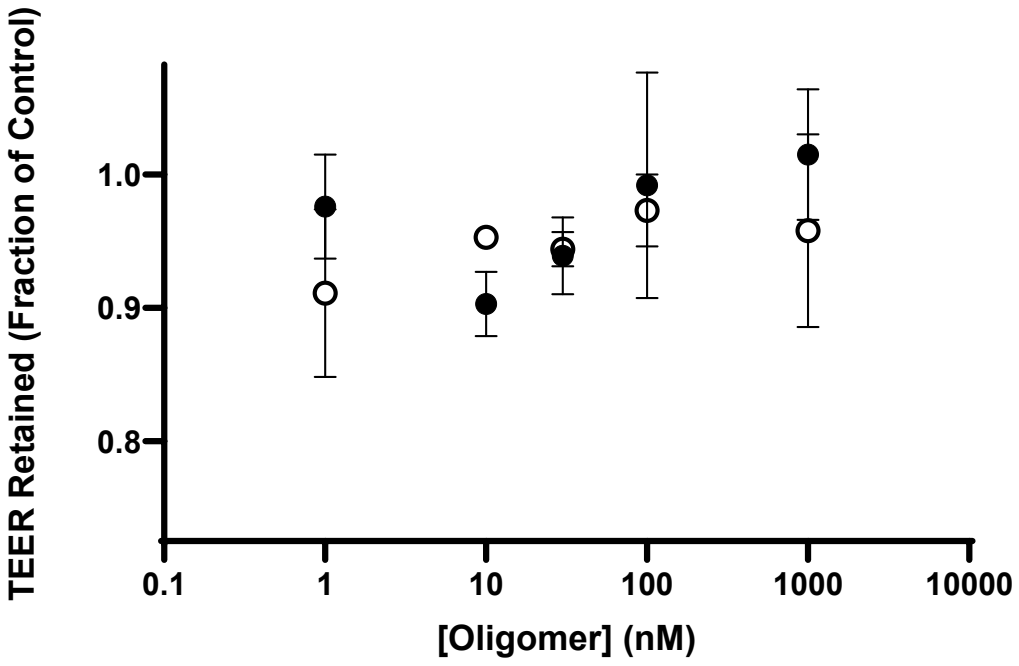

Figure 4.3 Comparison of Fraction of TEER retained after 24 h and 48 h oligomer treatment. The Confluent HBMVECs were treated with $A\beta_{1\text{-}42}$ oligomers at concentrations of 1-1000 nM. TEER was measured 24 (●) and 48 (○) h after treatment. Results reveal that 48 h treatment renders a larger response. Values are reported as the fraction of TEER observed prior to treatment. Error bars represent SEM, n = 3-4.

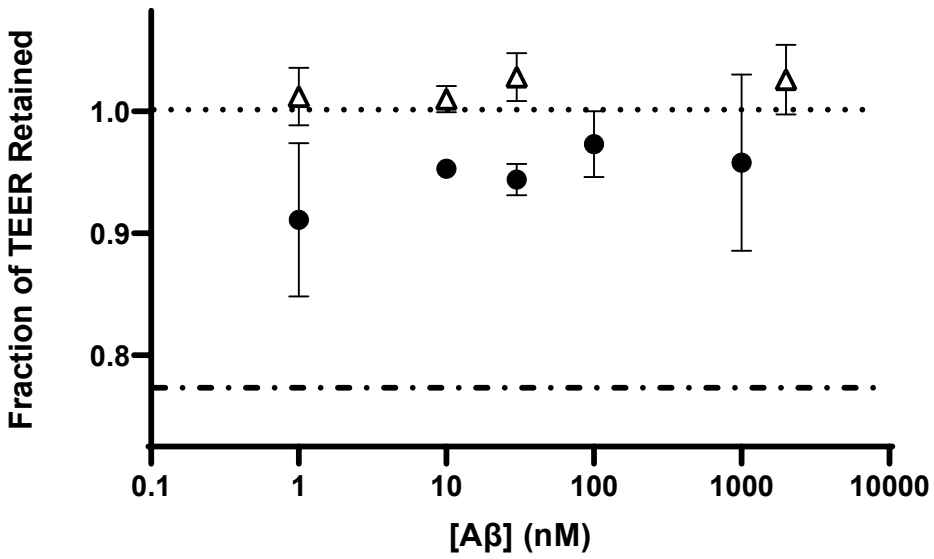

Figure 4.4. Oligomer treatment decreases TEER while monomer treatment renders TEER unchanged. Confluent HBMVECs were treated with Aβ1-42 oligomers (●) or SEC-isolated Aβ1-40 monomer (△) at concentrations of 0 (···) or 1-2000 nM. Treatment with TNF-α served as a positive control (·-·). TEER was measured 48 h after treatment. Values are reported as the fraction of TEER observed prior to treatment. Error bars represent SEM, n = 3-4; some error bars lie within symbols.

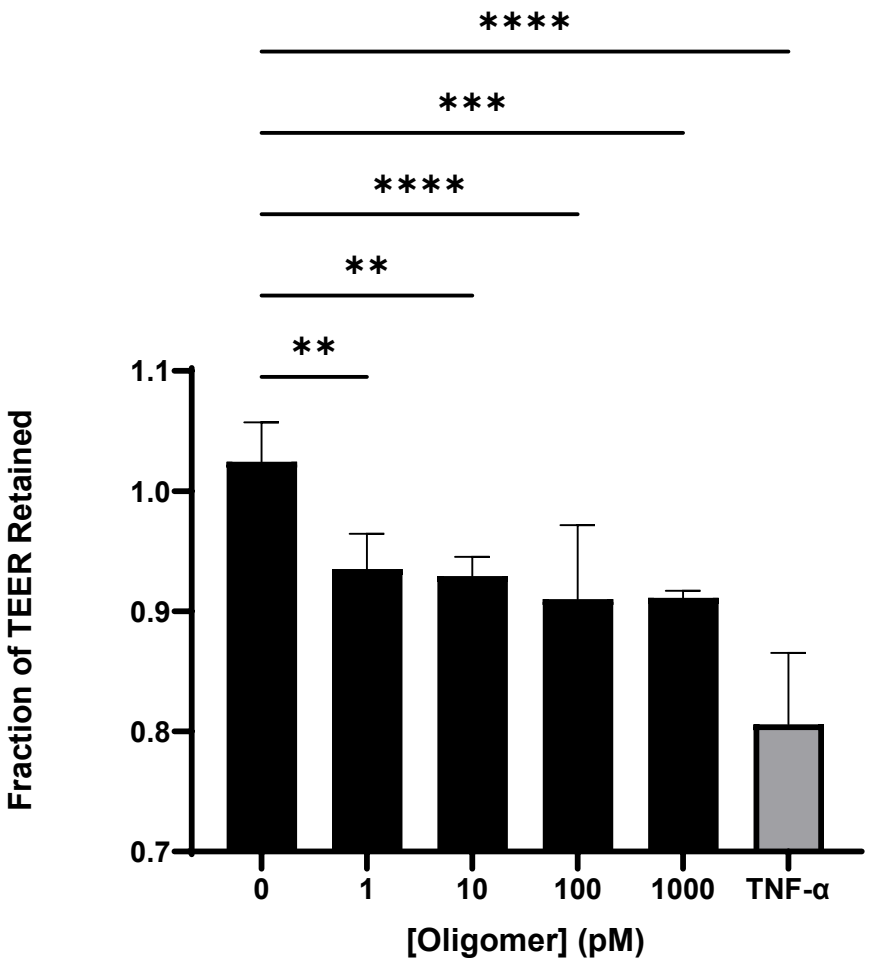

Figure 4.5. Picomolar concentrations of Aβ oligomers compromise TEER. Confluent HBMVECs were treated with 0 (negative control), 1, 10, 100, or 1000 pM $A\beta_{1\text{-}42}$, or a positive control of 20 units/mL of TNF-α. TEER was measured 48 h after treatment. Results are reported in as a fraction of TEER retained prior to treatment. Error bars indicate SEM, n = 3-4. **** $p < 0.0001$ *** $p < 0.0005$ ** $p < 0.01$

Chapter 5:

Sensitizing Endothelial Monolayers to Enhance Aβ Oligomeric Response

5.1 Introduction

With the goal of translating this experimental assay into a means for early AD detection, a more pronounced electrical response is preferred. To elicit this response two alternative routes were investigated: amplification of oligomeric Aβ and cellular monolayer sensitization.

First, investigations to amplify existing oligomer concentrations in samples were sought. We tried to exploit the nucleation dependent nature of amyloid protein aggregation, in which the lag time of aggregation for monomeric amyloid protein alone is abolished in the presence of aggregates.[25] We hypothesized that secondary nucleation could be induced by adding synthetic $A\beta_{1-40}$ monomer to samples containing $A\beta_{1-42}$ oligomers. The notion was if oligomeric protein is absent in the sample, synthetic monomer will remain inert and samples containing oligomers would yield more pronounced cellular TEER reduction. However, results indicated that the addition of monomeric Aβ to low concentrations of oligomers did not further reduce TEER as hypothesized. Therefore, other avenues were investigated.

To further explore if there is a method in which the cellular response to Aβ oligomers can be exacerbated, the sensitization of monolayers with a common ROS,

H_2O_2 was tested. Evidence suggests that one mechanism causing cognitive aging and AD is oxidative stress.[64] Oxidative stress results from an imbalance in the pro- oxidant/antioxidant homeostasis leading to the generation of toxic ROS. While ROS are necessary for cellular function, high levels are toxic to cells.[64] Oxidative damage to lipids, proteins, and DNA precede cell death by a various mechanisms, either by disabling crucial processes or upregulating toxic cascades.[65]

In AD, upregulation of nicotinamide adenine dinucleotide phosphate oxidase (Nox) results in the excess of superoxide (O_2^-), which undergoes spontaneous and enzymatic dismutation by superoxide dismutases (SOD), and results in an increase of a H_2O_2 byproduct.[66] *In vitro,* H_2O_2 is the most common means of ROS induction.[64,67] There is a concentration dependent effect of H_2O_2 on regulating permeability, angiogenesis, and cell viability. Higher concentrations can cause cell death and apoptosis.

The first goal of this study was to identify a concentration that did not induce a TEER reduction alone when treating cells for 24 h. HBMVECs were treated with a range of concentrations of H_2O_2 taken from the literature and TEER response was evaluated. After the concentration that did not significantly reduce TEER was selected, the second goal of this study was to determine if the addition of oligomeric Aβ would exacerbate the TEER decrease observed in prior studies where cells were treated with only oligomers.

5.2 Materials and Methods

5.2.1 Monolayer sensitization

Cells were grown and maintained as detailed in section 2.2. Monolayers of HBMVECs were prepared as described in Section 3.3. To determine a concentration of

H_2O_2 that alone did not affect the TEER measurements a range of concentrations were explored. A starting H_2O_2 concentration of 9.8 M was serial diluted to 0.01, 0.1, and 1.0 mM. Cells were treated apically with 0.01, 0.1, 1 mM H_2O_2. TEER was measured 24 hours after experiments.

5.2.2 Aβ preparation

Oligomers were prepared as detailed in section 3.4. After the 30-minute oligomerization, the reaction was halted by diluting with 1% FBS, 550 nM HC endothelial cell medium with or without 0.01 mM H_2O_2. Oligomers were diluted to a 1 and 10 pM concentrations. Immediately after dilution oligomers were administered apically to HBMVEC monolayers. TEER was measured after 48 h.

5.2.3 Statistical analysis

GraphPad Prism 9.0 software was used to analyze data obtained from cell sensitization and oligomeric Aβ treatments. Generated data for each concentration of H_2O_2 was analyzed for statistical significance via one-way ANOVA wherein each concentration was compared to the vehicle (0 mM). For the sensitized Aβ oligomer treatment, generated data for each concentration was analyzed for statistical significance via two-way ANOVA with multiple comparisons wherein the sensitized treatments were compared to the sensitized negative control (0 pM).

5.3 Results

5.3.1 Monolayer sensitization

Before treating cells, a range of concentrations of H2O2 were chosen based on the literature. Cells treated with 0.01, 0.1, and 1 mM H_2O_2 showed a concentration dependent

decrease for the 0.1 and 1 mM concentrations. The 1 mM and 0.01 mM concentrations decreased by 30.3% and 10.1% respectively. The 0.01 mM concentrations did not significantly decrease the TEER (Figure 5.1). Therefore, the 0.01 mM concentration was chosen to sensitize the monolayer in combination with oligomers.

5.3.2 Cell sensitization and oligomer treatment

Monolayers were treated simultaneously with 1 or 10 ρM oligomers and 0.01 mM H_2O_2. TEER was measured 48 h after treatment. When compared to sensitized monolayers not treated with $A\beta_{1-42}$ the 1 and 10 ρM concentrations both significantly reduced TEER to a retained percentage of 85.0 and 86.4%, respectively (Figure 5.2). This combined effect was more pronounced than the oligomer treatment alone.

5.4 Discussion

AD is not a closed loop system, and multiple mechanisms that are affected by the disease. Both oxidative stress and Aβ have been shown to intensify the endothelial cell response, leading to BBB dysfunction and contributing to the pathogenesis of AD.[18,64] Studies have shown that in an AD brain regions where there are elevated levels of Aβ also have increased levels of oxidative stress markers, including oxidation products from proteins, lipids, and nucleic acids. In contrast, brain regions with low Aβ levels do not present high concentrations of these markers.[68]

Endothelial dysfunction is linked to excess production of ROS.[66,67] Oxidative stress resulting from an imbalance between ROS and antioxidants can damage the endothelial cells of the BBB, leading to activation of inflammatory pathways and cell death, further exacerbating brain damage.[64] This, in turn, can led to increased

permeability of the BBB increasing the neurodegenerative process.[69] In studies of mice with Alzheimer-like pathologies, enhanced oxidative stress is an early development seen in the disease.[70] Incubating neurons with $A\beta_{1-42}$ leads to lipid peroxidation resulting in H_2O_2 as marked by protein bound 4-hydroxy-2-trans-nonenal (HNE).[71] However, there is a concentration dependent effect of H_2O_2 on regulating permeability, angiogenesis, and cell viability, and higher concentrations can cause cell death and apoptosis. It has been reported that low concentration of H_2O_2, 1 μM, does not disrupt tight junction proteins of microvascular endothelial cells, but a higher concentration such as 100 μM does induced disruption.[66] To find a concentration that did not induce large disruption, but just slightly stimulated HBMVECs, a range of concentrations were explored. A significantly large cellular disruption is seen with both 1 and 0.1 mM H_2O_2, which correlated with the concentration of stimulant (Figure 6.1). The 0.01 mM concentration of H_2O_2 did not cause a reduction in the fraction of TEER retained, but there is not as much of an increased fraction of TEER retained compared to the cells treated with the negative control (0 nM). Therefore, the 0.01 mM concentration of H_2O_2 was chosen for further experimentation.

Monolayers were stimulated with H_2O_2 and treated with $A\beta_{1-42}$ oligomers simultaneously. A simultaneous treatment is more representative of the disease state, where both oxidative stress and Aβ aggregation and accumulation are happening. Results indicated that the influence of oxidative stress in AD works in tandem with the toxicity of oligomeric Aβ. When stimulated and treated with $A\beta_{1-42}$ oligomers, cells had a more pronounced response compared to HBMVECs treated with oligomers alone,

demonstrated by the reduction of TEER. These findings highlight the interplay between oxidative stress, Aβ, and endothelial cell function in the development of AD.

By mildly stimulating the HBMVECs by adding low concentrations of H_2O_2, we were able to establish a threshold of concentrations that did not induce a TEER reduction but stimulated the cells in conjunction with oligomeric Aβ. In addition to giving a better understanding of how both oxidative stress and Aβ compromise the BBB, these results also reveal that the known physiological phenomenon of oxidative stress in AD can be leveraged to yield a more pronounced electrical response of HBMVECs to increase sensitivity for detection.

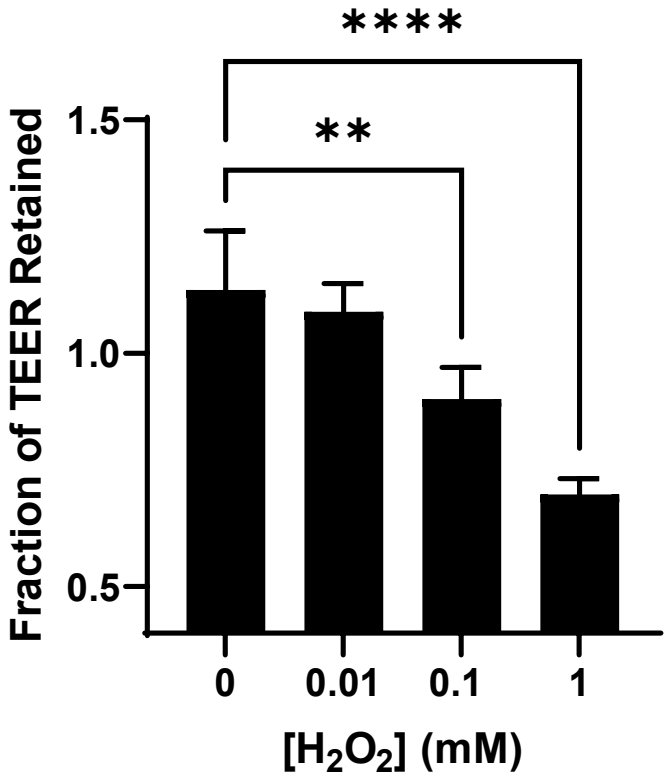

Figure 5.1 Low concentrations of H_2O_2 do not compromise TEER. Confluent HBMVECs were treated with 0.01, 0.1, and 1 mM H_2O_2. the 0.1 and 1 mM concentrations significantly reduce TEER, but not 0.01 mM H_2O_2.. Results are reported in as a fraction of TEER retained prior to stimulation. Error bars indicate SD, n = 3-4. **** $p < 0.0001$ ** $p < 0.005$.

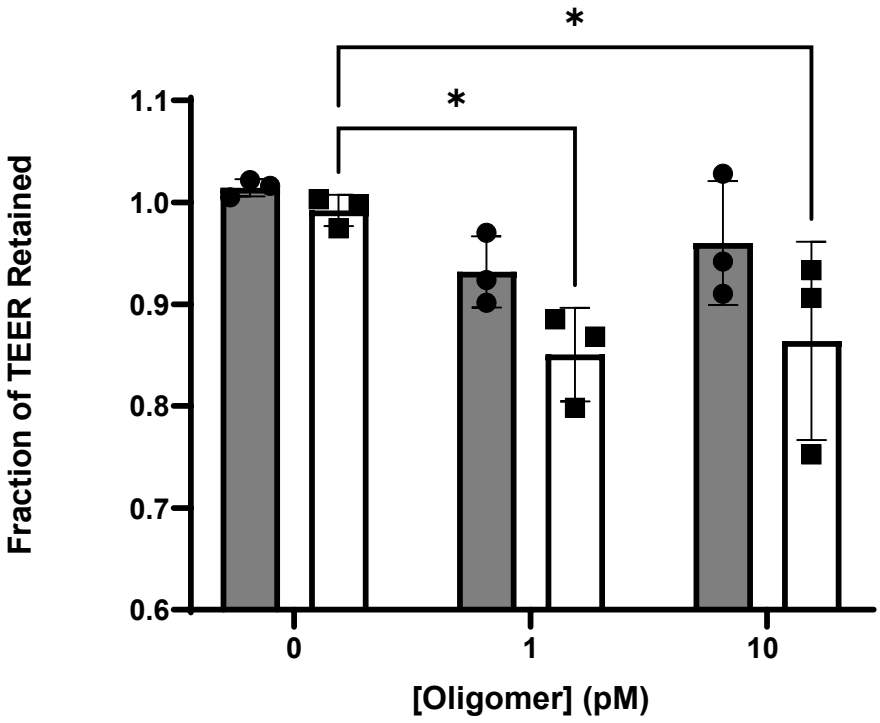

Figure 5.2 Sensitized HBMVECs have a more pronounced TEER reduction following Aβ oligomer treatment. Confluent HBMVECs were treated with 0 (●) or 0.01 mM H_2O_2 (■) and 1 or 10 pM $A\beta_{1\text{-}42}$ oligomers. TEER was measured 48 h after treatment. Results are reported as a fraction of TEER retained prior to treatment. Error bars indicate SEM, n = 3-4. * $p < 0.05$

Chapter 6: Conclusions

The work has rendered an *in vitro* cellular model representative of the BBB. A polycarbonate semipermeable membrane coated with bovine plasma fibronectin, rewetted with medium at least 1 h prior to cell seeding was chosen for cell seeding. Using a seeding density of 50,000 cells/well and reducing the medium from 5% to 1% FBS 3 days post-seeding further optimized the model for testing.

Using the established model, the electrical effect of the toxic form of Aβ, oligomers was explored. This work has shown that Aβ oligomers induce breakdown of HBMVEC monolayers, reducing their electrical resistance. Towards leveraging this response for early detection of AD, results demonstrated that Aβ oligomers alone induce a significant decrease in TEER, at a range of concentrations including physiological levels, while inert Aβ monomer has no effect on TEER. This work validates that the earliest Aβ aggregates induce an easily measurable endothelial permeability response.

Further, additional work has validated that sensitizing the endothelial monolayers with H_2O_2 simultaneously with Aβ oligomer treatment enables a more pronounced response. Towards leveraging a cell-based sensor for pre-symptomatic AD detection, results indicated that stimulating cells does further induce a larger TEER reduction in the presence of Aβ oligomers. Additionally, results also give insight to physiological

implications in AD, and how oxidative stress further induce the effect of oligomeric Aβ. This data provides a conceptual basis for the design of a cell-based biosensor for early AD detection that leverages selective BBB breakdown by small Aβ aggregates. This data also reveals how oxidative stress works in conjunction with the toxicity of Aβ oligomers.

Chapter 7: Future Work

7.1 Potential research avenues

This work has validated that physiological concentrations of $A\beta_{1-42}$ oligomers cause a significant decrease in HBMVECs' TEER measurements. To translate this experimental assay to a means for detection will require ensuring this assay will work in a physiological sample of CSF. Once confirmed that a similar result can been seen with CSF, then patient samples will be tested. Once validated, moving this assay to a chip-based approach should be considered.

Taking that Aβ is a part of the amyloid family which share the same conformational homology, it would be interesting to investigate other amyloid proteins and their effects of HBMVECs. These proteins share similar aggregation kinetics and β-sheet structures. Investigation into if other members of the amyloid family do induce a decrease in TEER of HBMVECs would offer insight to relating these proteins and finding commonality among the diseases that they characterize.

Recommendations for taking this experimental assay closer to a reproducible means for detection and other amyloid proteins that could elucidate a similar electrical response are detailed in this Chapter.

7.2 Translating measurements to patient samples

Transforming this experimental set up from Aβ spiked cell culture media to CSF samples containing Aβ will bring this experimental platform closer to a clinically available method for early detection. HBMVECs are quite sensitive to their environment, and to switch from a controlled medium to CSF which is slightly alkaline may pose challenges; therefore, testing the cellular response to CSF a must be observed.

7.2.1 Validation of model with CSF

To ensure that changes in TEER, permeability, and TJs are due to the Aβ in the samples and not from the CSF itself, cells will be treated with purchased CSF diluted in cell culture medium. Next, to ensure that a cellular response to oligomeric Aβ in CSF samples is observable, the cellular response will be investigated.

Before treating cells with patient samples, experiments should be conducted with CSF samples from healthy subjects to ensure that CSF alone does not cause unwarranted results from the cells. Cells will be grown and TEER will be followed until optimal TEER is reached. Cells treated with CSF diluted in cell culture medium with and without H_2O_2 and TEER observed. If there is not a reduction in TEER, further testing will be executed as described below. If the diluted CSF samples induce a reduction in TEER, then additional dilution with cell culture will be implemented and repeated experiments performed.

To confirm that Aβ oligomers in CSF samples will induce a change in the cellular monolayer, CSF will be doped with physiological concentrations synthetic of $A\beta_{1\text{-}42}$ oligomers, and TEER measurements will be monitored. Physiological concentrations of

monomer will serve as a control. Anticipated results are that CSF samples containing only monomeric Aβ will have no reduction in TEER, and the oligomeric samples will display a TEER reduction, with a more pronounced response seen in sensitized monolayers.

7.2.2 Translating measurements to CSF samples

Utilizing the sensitization protocol will help to determine if AD patient samples induce an observable response compared to samples from healthy patients. A manageable sample size is needed to validate this method for detection of oligomeric Aβ.

To achieve a more pronounced response, cells will be simultaneous treated with patient samples and H_2O_2, and TEER measurements will be observed at the optimal time previously established. TEER changes should be able to infer if there is a presence of Aβ oligomers in the sample. It is hypothesized that TEER measurements of cells sensitized and incubated with CSF samples will distinguish AD patients and healthy subjects.

Power calculations were performed to determine the minimum number of patient samples for an adequate study power. The statistical parameters to determine the sample size were anticipated means of 1 ± 0.1 fraction of TEER retained for oligomer negative patient samples. Oligomer positive patients samples would have at least a decrease of at least 10% in TEER after cell treatment for a fraction of TEER retained being less than or equal to 0.9.[72] With type I error, or α, fixed at 0.05 and type II error, or β, fixed at a level of 0.20, meaning that there is a less than 20% chance of a false-negative conclusion, the resulting minimum sample size is a total of 8 patient samples. To further reduce error, 12 patient samples will be used for this study, 6 healthy and 6 diagnosed with AD.

Patient samples will be provided by a local physician at Southeastern Neurology and Memory Clinic. Samples are from patients participating in a longitudinal study for AD and dementia. Samples were taken from patients genetically predisposition for AD by being a carrier for the APOE4 gene, patients who have familial history of AD, and patients without a known relation to the disease. Along with providing CSF samples, blood samples and a series of cognitive test were periodically acquired and followed by the Clinic. To test for the presence of Aβ oligomers in patient samples, the samples will be diluted with cell culture media containing H_2O_2, and introduced to HBMVEC monolayers. TEER measurements will be taken at the optimal time established above.

7.3 Characterization of the endothelial cellular response to other amyloid proteins

Over 30 unrelated proteins are known to form amyloid fibrils in vivo.[73,74] Amyloidosis is a clinical disorder caused by extracellular deposition of amyloid fibrils that originate from aggregation of misfolded proteins that are soluble as monomers. The defining structural feature of amyloid proteins occurs from the cross-β fold that aggregates share.[75] Aβ aggregates interact with endothelial cell surface receptors that are pattern recognition receptors, such as, RAGE and the low-density lipoprotein receptor-related protein (LRP)-1.[76] These receptors recognize the conformation of the β-plated sheet rather than the protein sequence suggesting that other amyloid proteins could elicit similar cellular responses seen with Aβ. It is hypothesized that due to the conformational homology among amyloid proteins, similar endothelial cellular responses to aggregates are expected.

Work toward this hypothesis could entail testing of the physiological activity of oligomers utilizing the protocol developed for Aβ to demonstrate an endothelial cells

response to α-synuclein, insulin, amylin, and atrial natriuretic peptide oligomers. Oligomers of each protein will then be introduced to cellular monolayers, and TEER will be measured. TEER investigations and breakdown of tight junctions by oligomers of each of these amyloid proteins will determine whether oligomeric forms of other amyloid proteins elicit the same reduction in TEER observed with Aβ. This work will demonstrate, for the first time, a generalization of the endothelial permeability cellular response among different amyloid proteins and validate a means for detection of multiple amyloid oligomers. A few diseases that are characterized by amyloid aggregation are described below.

7.3.1 Parkinson's disease

Parkinson's disease (PD) is a neurodegenerative disease with outward symptoms of bradykinesia, rigidity, and rest temors.[77] Pathologically, the main hallmark in PD is the presences of Lewy bodies (LBs) and Lewy neurites (LNs) in the brain, which are made of aggregated α-synuclein, a presynaptic protein.[78] Aggregation of α-synuclein is pathogenic and related to the propagation to the disease.[79] Soluble oligomers of α-synuclein disrupt cellular homeostasis and cause neuronal death, through multiple intracellular targets[79], and can enhance membrane permeability.[75] Oligomeric α-synuclein detection would assist in early disease detection for PD.

7.3.2 Type II diabetes

Amylin hormone, also known as islet amyloid polypeptide (IAPP), is co-secreted with insulin from the pancreatic β-cells.[80] Aggregates of IAPP inhibit the activity of insulin and glucagon leading to the cause type 2 diabetes mellitus (TDM2).[80] In the

disease, aggregated IAPP is frequently present in the Islets of Langerhans in diabetics patients, but not universally.[73] In autopsy studies, amyloid in the pancreatic islets has been detected 50-90% more frequently in patients with TDM2[81]. Studies have shown that IAPP fibril formation can cause death of β-cells by inducing apoptosis, and the oligomers of the peptides are considered the most detrimental to cell viability[81], similarly thought in AD. While apoptosis of β-cells has been identified the vascular effects aggregated amylin have not. Detection of the presence of IAPP oligomers could help with early diagnosis of TDM2 and provide information of the vascular effects of TDM2.

7.3.3 Insulin-derived amyloidosis

Similarly, insulin derived amyloidosis arises from amyloid aggregation in insulin therapies. It can cause a rigid subcutaneous mass at the site of injection, resulting in injection site inflammation. Unpredictable release of insulin within the mass is a risk of this aggregation and can be dangerous for diabetic patients by causing unstable blood glucose levels and severe hypoglycemia.[82] While this protein has a native structure in pharmaceutical production processing it can become unfolded which can lead to misfolding and aggregation. Detecting aggregated insulin would allow bad batches of insulin to be removed from pharmaceutical production incidentally reducing the risk of insulin-derived amyloidosis for insulin dependent patients.

7.3.4 Atrial amyloidosis

Cardiac atrial amyloidosis (CAA) is characterized by the deposition of amyloid throughout the myocardium[83]. Atrial natriuretic peptide (ANP) is a normal hormone secreted by cardiomyocytes, but in cardiac amyloidosis it aggregates and deposits.

Isolated CAA is associated with dysrhythmia following cardiac surgery. The detection of oligomeric ANP prior to patient surgery could offer insight into post-operation therapeutics for patients and doctors.[77]

References

1 Association, A. s. 2022 Alzheimer's Disease Facts and Figures. *Alzheimers Dement* **18** (2022).

2 Kumfor, F., Halliday, G. M. & Piguet, O. Clinical Aspects of Alzheimer's Disease. *Adv Neurobiol* **15**, 31-53, doi:10.1007/978-3-319-57193-5_2 (2017).

3 Marcus, C., Mena, E. & Subramaniam, R. M. Brain PET in the diagnosis of Alzheimer's disease. *Clin Nucl Med* **39**, e413-422; quiz e423-416, doi:10.1097/RLU.0000000000000547 (2014).

4 Kirova, A. M., Bays, R. B. & Lagalwar, S. Working memory and executive function decline across normal aging, mild cognitive impairment, and Alzheimer's disease. *Biomed Res Int* **2015**, 748212, doi:10.1155/2015/748212 (2015).

5 Athar, T., Al Balushi, K. & Khan, S. A. Recent advances on drug development and emerging therapeutic agents for Alzheimer's disease. *Mol Biol Rep* **48**, 5629-5645, doi:10.1007/s11033-021-06512-9 (2021).

6 Ferreira-Vieira, T. H., Guimaraes, I. M., Silva, F. R. & Ribeiro, F. M. Alzheimer's disease: Targeting the Cholinergic System. *Curr Neuropharmacol* **14**, 101-115, doi:10.2174/1570159x13666150716165726 (2016).

7 Khan, S., Barve, K. H. & Kumar, M. S. Recent Advancements in Pathogenesis, Diagnostics and Treatment of Alzheimer's Disease. *Curr Neuropharmacol* **18**, 1106-1125, doi:10.2174/1570159X18666200528142429 (2020).

8 Liu, P. P., Xie, Y., Meng, X. Y. & Kang, J. S. History and progress of hypotheses and clinical trials for Alzheimer's disease. *Signal Transduct Target Ther* **4**, 29, doi:10.1038/s41392-019-0063-8 (2019).

9 Zenaro, E., Piacentino, G. & Constantin, G. The blood-brain barrier in Alzheimer's disease. *Neurobiol Dis* **107**, 41-56, doi:10.1016/j.nbd.2016.07.007 (2017).

10 O'Brien, R. J. & Wong, P. C. Amyloid precursor protein processing and Alzheimer's disease. *Annu Rev Neurosci* **34**, 185-204, doi:10.1146/annurev-neuro-061010-113613 (2011).

11 Minter, M. R., Taylor, J. M. & Crack, P. J. The contribution of neuroinflammation to amyloid toxicity in Alzheimer's disease. *J Neurochem* **136**, 457-474, doi:10.1111/jnc.13411 (2016).

12 Ding, Y. *et al.* Amyloid Beta Oligomers Target to Extracellular and Intracellular Neuronal Synaptic Proteins in Alzheimer's Disease. *Front Neurol* **10**, 1140, doi:10.3389/fneur.2019.01140 (2019).

13 Sweeney, M. D., Sagare, A. P. & Zlokovic, B. V. Blood-brain barrier breakdown in Alzheimer disease and other neurodegenerative disorders. *Nat Rev Neurol* **14**, 133-150, doi:10.1038/nrneurol.2017.188 (2018).

14 Parodi-Rullan, R., Sone, J. Y. & Fossati, S. Endothelial Mitochondrial Dysfunction in Cerebral Amyloid Angiopathy and Alzheimer's Disease. *J Alzheimers Dis* **72**, 1019-1039, doi:10.3233/JAD-190357 (2019).

15 Martinez-Morillo, E. *et al.* Total apolipoprotein E levels and specific isoform composition in cerebrospinal fluid and plasma from Alzheimer's disease patients and controls. *Acta Neuropathol* **127**, 633-643, doi:10.1007/s00401-014-1266-2 (2014).

16 Mila-Aloma, M., Suarez-Calvet, M. & Molinuevo, J. L. Latest advances in cerebrospinal fluid and blood biomarkers of Alzheimer's disease. *Ther Adv Neurol Disord* **12**, 1756286419888819, doi:10.1177/1756286419888819 (2019).

17 Ramos-Cejudo, J. *et al.* Traumatic Brain Injury and Alzheimer's Disease: The Cerebrovascular Link. *EBioMedicine* **28**, 21-30, doi:10.1016/j.ebiom.2018.01.021 (2018).

18 Li, J. *et al.* Vascular risk factors promote conversion from mild cognitive impairment to Alzheimer disease. *Neurology* **76**, 1485-1491, doi:10.1212/WNL.0b013e318217e7a4 (2011).

19 Porsteinsson, A. P., Isaacson, R. S., Knox, S., Sabbagh, M. N. & Rubino, I. Diagnosis of Early Alzheimer's Disease: Clinical Practice in 2021. *The Journal Of Prevention of Alzheimer's Disease*, 1-16, doi:10.14283/jpad.2021.23 (2021).

20 Gauthreaux, K. *et al.* Concordance of Clinical Alzheimer Diagnosis and Neuropathological Features at Autopsy. *J Neuropathol Exp Neurol* **79**, 465-473, doi:10.1093/jnen/nlaa014 (2020).

21 Hardy, J. & Allsop, D. Amyloid deposition as the central event in the aetiology of Alzheimer's disease. *Trends Pharmacol Sci* **12**, 383-388, doi:10.1016/0165-6147(91)90609-v (1991).

22 Eisenberg, D. & Jucker, M. The amyloid state of proteins in human diseases. *Cell* **148**, 1188-1203, doi:10.1016/j.cell.2012.02.022 (2012).

23 Chen, G. F. *et al.* Amyloid beta: structure, biology and structure-based therapeutic development. *Acta Pharmacol Sin* **38**, 1205-1235, doi:10.1038/aps.2017.28 (2017).

24 Zhao, J., Liu, X., Xia, W., Zhang, Y. & Wang, C. Targeting Amyloidogenic Processing of APP in Alzheimer's Disease. *Front Mol Neurosci* **13**, 137, doi:10.3389/fnmol.2020.00137 (2020).

25 Linse, S. Monomer-dependent secondary nucleation in amyloid formation. *Biophys Rev* **9**, 329-338, doi:10.1007/s12551-017-0289-z (2017).

26 Tornquist, M. *et al.* Secondary nucleation in amyloid formation. *Chem Commun (Camb)* **54**, 8667-8684, doi:10.1039/c8cc02204f (2018).

27 Shulman, R. G., Hyder, F. & Rothman, D. L. Cerebral metabolism and consciousness. *Comptes Rendus Biologies* **326**, 253-273, doi:10.1016/s1631-0691(03)00071-4 (2003).

28 Maiuolo, J. *et al.* The "Frail" Brain Blood Barrier in Neurodegenerative Diseases: Role of Early Disruption of Endothelial Cell-to-Cell Connections. *Int J Mol Sci* **19**, doi:10.3390/ijms19092693 (2018).

29 Serlin, Y., Shelef, I., Knyazer, B. & Friedman, A. Anatomy and physiology of the blood-brain barrier. *Semin Cell Dev Biol* **38**, 2-6, doi:10.1016/j.semcdb.2015.01.002 (2015).

30 Daneman, R. & Prat, A. The blood-brain barrier. *Cold Spring Harb Perspect Biol* **7**, a020412, doi:10.1101/cshperspect.a020412 (2015).

31 Aday, S., Cecchelli, R., Hallier-Vanuxeem, D., Dehouck, M. P. & Ferreira, L. Stem Cell-Based Human Blood-Brain Barrier Models for Drug Discovery and Delivery. *Trends Biotechnol* **34**, 382-393, doi:10.1016/j.tibtech.2016.01.001 (2016).

32 González-Mariscal, L., Betanzos, A., Nava, P. & Jaramillo, B. E. Tight junction proteins. *Progress in Biophysics and Molecular Biology* **81**, 1-44, doi:10.1016/s0079-6107(02)00037-8 (2003).

33 Langen, U. H., Ayloo, S. & Gu, C. Development and Cell Biology of the Blood-Brain Barrier. *Annu Rev Cell Dev Biol* **35**, 591-613, doi:10.1146/annurev-cellbio-100617-062608 (2019).

34 Hudson, N. & Campbell, M. Tight Junctions of the Neurovascular Unit. *Front Mol Neurosci* **14**, 752781, doi:10.3389/fnmol.2021.752781 (2021).

35 Schaeffer, S. & Iadecola, C. Revisiting the neurovascular unit. *Nat Neurosci* **24**, 1198-1209, doi:10.1038/s41593-021-00904-7 (2021).

36 Helms, H. C. *et al.* In vitro models of the blood-brain barrier: An overview of commonly used brain endothelial cell culture models and guidelines for their use. *J Cereb Blood Flow Metab* **36**, 862-890, doi:10.1177/0271678X16630991 (2016).

37 Cipolla, M. J. in *The Cerebral Circulation Integrated Systems Physiology: From Molecule to Function* Ch. 2Anato my and Ultrastructure, (Morgan & Claypool Life Sciences, 2009).

38 Bell, A. H., Miller, S. L., Castillo-Melendez, M. & Malhotra, A. The Neurovascular Unit: Effects of Brain Insults During the Perinatal Period. *Front Neurosci* **13**, 1452, doi:10.3389/fnins.2019.01452 (2019).

39 Greenberg, S. M. *et al.* Cerebral amyloid angiopathy and Alzheimer disease - one peptide, two pathways. *Nat Rev Neurol* **16**, 30-42, doi:10.1038/s41582-019-0281-2 (2020).

40 Sagare, A. P., Bell, R. D. & Zlokovic, B. V. Neurovascular dysfunction and faulty amyloid beta-peptide clearance in Alzheimer disease. *Cold Spring Harb Perspect Med* **2**, doi:10.1101/cshperspect.a011452 (2012).

41 Gastfriend, B. D., Palecek, S. P. & Shusta, E. V. Modeling the blood-brain barrier: Beyond the endothelial cells. *Curr Opin Biomed Eng* **5**, 6-12, doi:10.1016/j.cobme.2017.11.002 (2018).

42 Ramachandran, B., Chakraborty, S., Dixit, M. & Muthuvijayan, V. A comparative study of polyethylene terephthalate surface carboxylation techniques: Characterization, in vitro haemocompatibility and endothelialization. *Reactive and Functional Polymers* **122**, 22-32, doi:10.1016/j.reactfunctpolym.2017.11.001 (2018).

43 Feinkohl, I. *et al.* Plasma Amyloid Concentration in Alzheimer's Disease: Performance of a High-Throughput Amyloid Assay in Distinguishing Alzheimer's Disease Cases from Controls. *J Alzheimers Dis* **74**, 1285-1294, doi:10.3233/JAD-200046 (2020).

44 Schindler, S. E. *et al.* High-precision plasma beta-amyloid 42/40 predicts current and future brain amyloidosis. *Neurology*, doi:10.1212/WNL.0000000000008081 (2019).

45 Lazzari, C., Kipanyula, M. J., Agostini, M., Pozzan, T. & Fasolato, C. Abeta42 oligomers selectively disrupt neuronal calcium release. *Neurobiol Aging* **36**, 877-885, doi:10.1016/j.neurobiolaging.2014.10.020 (2015).

46 Marzano, M. *et al.* Studying the Inflammatory Responses to Amyloid Beta Oligomers in Brain-Specific Pericyte and Endothelial Co-culture from Human Stem Cells. *Front Chem Eng* **4**, doi:10.3389/fceng.2022.927188 (2022).

47 Fonseca, A. C., Ferreiro, E., Oliveira, C. R., Cardoso, S. M. & Pereira, C. F. Activation of the endoplasmic reticulum stress response by the amyloid-beta 1-40 peptide in brain endothelial cells. *Biochim Biophys Acta* **1832**, 2191-2203, doi:10.1016/j.bbadis.2013.08.007 (2013).

48 Gonzalez-Velasquez, F. J., Kotarek, J. A. & Moss, M. A. Soluble aggregates of the amyloid-beta protein selectively stimulate permeability in human brain microvascular endothelial monolayers. *J Neurochem* **107**, 466-477, doi:10.1111/j.1471-4159.2008.05618.x (2008).

49 Gonzalez-Velasquez, F. *et al.* Activation of brain endothelium by soluble aggregates of the amyloid-beta protein involves nuclear factor-kappaB. *Curr Alzheimer Res* **8**, 81-94, doi:10.2174/156720511794604606 (2011).

50 Daniel H. Elbrecht, C. J. L. a. J. J. H. Transepithelial/endothelial Electrical Resistance (TEER) theory and applications for microfluidic body-on-a-chip devices. doi:10.29245/2572-9411/2016/3.1026.

51 Maherally, Z. *et al.* Real-time acquisition of transendothelial electrical resistance in an all-human, in vitro, 3-dimensional, blood-brain barrier model exemplifies

tight-junction integrity. *FASEB J* **32**, 168-182, doi:10.1096/fj.201700162R (2018).

52 INSTRUMENTS, W.

53 <EVOM2_IM.pdf>.

54 Vigh, J. P. *et al.* Transendothelial Electrical Resistance Measurement across the Blood-Brain Barrier: A Critical Review of Methods. *Micromachines (Basel)* **12**, doi:10.3390/mi12060685 (2021).

55 Urich, E., Lazic, S. E., Molnos, J., Wells, I. & Freskgard, P. O. Transcriptional profiling of human brain endothelial cells reveals key properties crucial for predictive in vitro blood-brain barrier models. *PLoS One* **7**, e38149, doi:10.1371/journal.pone.0038149 (2012).

56 Furihata, T. *et al.* Hydrocortisone enhances the barrier properties of HBMEC/cibeta, a brain microvascular endothelial cell line, through mesenchymal-to-endothelial transition-like effects. *Fluids Barriers CNS* **12**, 7, doi:10.1186/s12987-015-0003-0 (2015).

57 Hoheisel, D. *et al.* Hydrocortisone reinforces the blood-brain barrier properties in a serum free cell culture system. *Biochem Biophys Res Commun* **244**, 312-316, doi:10.1006/bbrc.1997.8051 (1998).

58 Montagne, A. *et al.* Blood-brain barrier breakdown in the aging human hippocampus. *Neuron* **85**, 296-302, doi:10.1016/j.neuron.2014.12.032 (2015).

59 Abolhassani, N. *et al.* Molecular pathophysiology of impaired glucose metabolism, mitochondrial dysfunction, and oxidative DNA damage in

Alzheimer's disease brain. *Mech Ageing Dev* **161**, 95-104, doi:10.1016/j.mad.2016.05.005 (2017).

60 Gu, L. & Guo, Z. Alzheimer's Abeta42 and Abeta40 peptides form interlaced amyloid fibrils. *J Neurochem* **126**, 305-311, doi:10.1111/jnc.12202 (2013).

61 Yue, Q., Zhou, X., Zhang, Z. & Hoi, M. P. M. Murine Beta-Amyloid (1-42) Oligomers Disrupt Endothelial Barrier Integrity and VEGFR Signaling via Activating Astrocytes to Release Deleterious Soluble Factors. *Int J Mol Sci* **23**, doi:10.3390/ijms23031878 (2022).

62 Albensi, B. C. What Is Nuclear Factor Kappa B (NF-kappaB) Doing in and to the Mitochondrion? *Front Cell Dev Biol* **7**, 154, doi:10.3389/fcell.2019.00154 (2019).

63 Ciudad, S. *et al.* Abeta(1-42) tetramer and octamer structures reveal edge conductivity pores as a mechanism for membrane damage. *Nat Commun* **11**, 3014, doi:10.1038/s41467-020-16566-1 (2020).

64 Ionescu-Tucker, A. & Cotman, C. W. Emerging roles of oxidative stress in brain aging and Alzheimer's disease. *Neurobiol Aging* **107**, 86-95, doi:10.1016/j.neurobiolaging.2021.07.014 (2021).

65 Barnham, K. J., Masters, C. L. & Bush, A. I. Neurodegenerative diseases and oxidative stress. *Nat Rev Drug Discov* **3**, 205-214, doi:10.1038/nrd1330 (2004).

66 Alamu, O., Rado, M., Ekpo, O. & Fisher, D. Differential Sensitivity of Two Endothelial Cell Lines to Hydrogen Peroxide Toxicity: Relevance for In Vitro Studies of the Blood-Brain Barrier. *Cells* **9**, doi:10.3390/cells9020403 (2020).

67 Lee, H. S. *et al.* Hydrogen peroxide-induced alterations of tight junction proteins in bovine brain microvascular endothelial cells. *Microvasc Res* **68**, 231-238, doi:10.1016/j.mvr.2004.07.005 (2004).

68 Cheignon, C. *et al.* Oxidative stress and the amyloid beta peptide in Alzheimer's disease. *Redox Biol* **14**, 450-464, doi:10.1016/j.redox.2017.10.014 (2018).

69 Kitaguchi, H. *et al.* Chronic cerebral hypoperfusion accelerates amyloid beta deposition in APPSwInd transgenic mice. *Brain Res* **1294**, 202-210, doi:10.1016/j.brainres.2009.07.078 (2009).

70 Gu, F., Zhu, M., Shi, J., Hu, Y. & Zhao, Z. Enhanced oxidative stress is an early event during development of Alzheimer-like pathologies in presenilin conditional knock-out mice. *Neurosci Lett* **440**, 44-48, doi:10.1016/j.neulet.2008.05.050 (2008).

71 Mark, R. J., Lovell, M. A., Markesbery, W. R., Uchida, K. & Mattson, M. P. A role for 4-hydroxynonenal, an aldehydic product of lipid peroxidation, in disruption of ion homeostasis and neuronal death induced by amyloid beta-peptide. *J Neurochem* **68**, 255-264, doi:10.1046/j.1471-4159.1997.68010255.x (1997).

72 Noordzij, M., Dekker, F. W., Zoccali, C. & Jager, K. J. Sample size calculations. *Nephron Clin Pract* **118**, c319-323, doi:10.1159/000322830 (2011).

73 Pepys, M. B. Amyloidosis. *Annu Rev Med* **57**, 223-241, doi:10.1146/annurev.med.57.121304.131243 (2006).

74 Iadanza, M. G., Jackson, M. P., Hewitt, E. W., Ranson, N. A. & Radford, S. E. A new era for understanding amyloid structures and disease. *Nat Rev Mol Cell Biol* **19**, 755-773, doi:10.1038/s41580-018-0060-8 (2018).

75 Verma, M., Vats, A. & Taneja, V. Toxic species in amyloid disorders: Oligomers or mature fibrils. *Ann Indian Acad Neurol* **18**, 138-145, doi:10.4103/0972-2327.144284 (2015).

76 Donahue, J. E. *et al.* RAGE, LRP-1, and amyloid-beta protein in Alzheimer's disease. *Acta Neuropathol* **112**, 405-415, doi:10.1007/s00401-006-0115-3 (2006).

77 Davie, C. A. A review of Parkinson's disease. *Br Med Bull* **86**, 109-127, doi:10.1093/bmb/ldn013 (2008).

78 Ghosh, D., Mehra, S., Sahay, S., Singh, P. K. & Maji, S. K. alpha-synuclein aggregation and its modulation. *Int J Biol Macromol* **100**, 37-54, doi:10.1016/j.ijbiomac.2016.10.021 (2017).

79 Stefanis, L. alpha-Synuclein in Parkinson's disease. *Cold Spring Harb Perspect Med* **2**, a009399, doi:10.1101/cshperspect.a009399 (2012).

80 Paul, A., Kalita, S., Kalita, S., Sukumar, P. & Mandal, B. Disaggregation of Amylin Aggregate by Novel Conformationally Restricted Aminobenzoic Acid containing alpha/beta and alpha/gamma Hybrid Peptidomimetics. *Sci Rep* **7**, 40095, doi:10.1038/srep40095 (2017).

81 Hoppener, J. W. & Lips, C. J. Role of islet amyloid in type 2 diabetes mellitus. *Int J Biochem Cell Biol* **38**, 726-736, doi:10.1016/j.biocel.2005.12.009 (2006).

82 Gupta, Y., Singla, G. & Singla, R. Insulin-derived amyloidosis. *Indian J Endocrinol Metab* **19**, 174-177, doi:10.4103/2230-8210.146879 (2015).

83 Bhakhri, K. *et al.* Isolated atrial amyloid: a potential contributor to morbidity and mortality following cardiac surgery. *Interact Cardiovasc Thorac Surg*, doi:10.1093/icvts/ivz051 (2019).